

A Quantitative Theory of Bottleneck Structures for Data Networks

Technical Report, August 2021, New York, USA

Jordi Ros-Giralt¹, Noah Amsel², Sruthi Yellamraju³, James Ezick³, Richard Lethin³
Yuang Jiang⁴, Aosong Feng⁴, Leandros Tassioulas⁴

contact: jros@qti.qualcomm.com,

¹Qualcomm Europe, Inc

²Formerly of Qualcomm Technologies, Inc

³Qualcomm Technologies, Inc

⁴Yale, University

Abstract—The conventional view of the congestion control problem in data networks is based on the principle that a flow’s performance is uniquely determined by the state of its bottleneck link, regardless of the topological properties of the network. However, recent work has shown that the behavior of congestion-controlled networks is better explained by models that account for the interactions between bottleneck links. These interactions are captured by a latent *bottleneck structure*, a model describing the complex ripple effects that changes in one part of the network exert on the other parts. In this paper, we present a *quantitative* theory of bottleneck structures (QTBS), a mathematical and engineering framework comprising a family of polynomial-time algorithms that can be used to reason about a wide variety of network optimization problems, including routing, capacity planning and flow control. QTBS can contribute to traffic engineering by making clear predictions about the relative performance of alternative flow routes, and by providing numerical recommendations for the optimal rate settings of traffic shapers. A particularly novel result in the domain of capacity planning indicates that previously established rules for the design of folded-Clos networks are suboptimal when flows are congestion controlled. We show that QTBS can be used to derive the optimal rules for this important class of topologies, and empirically demonstrate the correctness and efficacy of these results using the BBR and Cubic congestion-control algorithms.

1. Introduction

Most research on the problem of congestion control for data networks is based on the principle that the performance of a flow is solely determined by the state of its bottleneck link. This view was presented in the original congestion control algorithm by Jacobson [1], which helped the Internet recover from congestion collapse in 1988, and it persisted throughout the more than 30 years of research and development that followed, including Google’s new BBR algorithm [2]. While it is certainly true that a flow’s performance is limited by the state of its bottleneck link, recent work

[3] reveals a deeper view of network behavior, describing how bottlenecks interact with each other through a latent structure—called the *bottleneck structure*—that depends on the topological, routing and flow control properties of the network. This latent structure explains how the performance of one bottleneck can affect other bottlenecks, and provides a framework to understand how perturbations in the capacity of a link or the rate of a flow propagate through a network, affecting other links and flows.

While [3] introduced the concept of bottleneck structure, the analysis provided was qualitative. In this paper we present a *quantitative theory of bottleneck structures* (QTBS), a mathematical framework that yields a set of polynomial time algorithms for quantifying the ripple effects of perturbations in a network. Perturbations can either be unintentional (such as the effect of a link failure or the sudden arrival of a large flow in a network) or intentional (such as the upgrade of a network link to a higher capacity or the modification of a route with the goal of optimizing performance). With QTBS, a network operator can quantify the effect of such perturbations and use this information to optimize network performance.

The theoretical contributions of this paper are as follows:

- A new generalized bottleneck structure called *gradient graph* is studied in detail. A key difference with the bottleneck structure introduced in [3] is that the gradient graph allows us to not only qualify the influences that flows and bottlenecks exert on each other, but also to quantify them. This leads to the development of a quantitative theory of bottleneck structures (QTBS), introduced in this paper. (Section 2.2)
- A novel, fast algorithm to compute the gradient graph is developed. This algorithm constitutes an asymptotic speed-up compared to those presented in [3], allowing us to scale our methodology to large production networks (Sections 2.2.)
- The concepts of *link* and *flow gradient* are introduced. These mathematical operators quantify the effects of infinitesimally small perturbations in a network, the core building blocks of QTBS. A new, fast method to effi-

ciently compute the gradients by leveraging the bottleneck structure is presented. (Section 2.3.)

Applications demonstrating the practical implications of QTBS are provided in the areas of routing, capacity planning and flow control. In each of these applications, we show how QTBS can potentially alter some of the established conventional best practices. Our practical contributions are as follows:

- In the routing application, we introduce an algorithm to find maximal-throughput routes by anticipating the effects of the congestion control algorithm. While in traditional traffic engineering approaches (e.g., [4]) the problems of routing and flow control are considered independently, we show how QTBS can help resolve them jointly, allowing operators to design routes that are efficient from a congestion control standpoint. (Section 3.1.)
- In the capacity planning application, we use QTBS to optimize the bandwidth allocation between the spine and leaf links of a fat-tree (also known as folded-Clos [5]). We demonstrate that, due to the effects of congestion control, the optimal design differs from the full fat-tree configuration proposed by Leiserson [6]. (Section 3.2.)
- In the flow control application, we show that QTBS can be used to precisely compute the rate reduction that a set of traffic shapers must impose on the network’s low priority flows in order to achieve a quantifiable positive impact on the high-priority flows. (Section 3.3.)
- To demonstrate that networks behave according to QTBS, we carry out experiments for each application we consider using production TCP/IP code and the widely adopted BBR [2] and Cubic [7] congestion control algorithms. (Section 3.)

2. Quantitative Theory of Bottleneck Structures (QTBS)

2.1. Network Model

In their simplest form, networks can be modeled using two kinds of elements: links, which are communication resources with a limited capacity; and flows, which make use of these communication resources. We formalize the definition of a network as follows:

Definition 1. Network. We say that a tuple $\mathcal{N} = \langle \mathcal{L}, \mathcal{F}, \{c_l, \forall l \in \mathcal{L}\} \rangle$ is a network if:

- \mathcal{L} is a set of links of the form $\{l_1, l_2, \dots, l_{|\mathcal{L}|}\}$,
- \mathcal{F} is a set of flows of the form $\{f_1, f_2, \dots, f_{|\mathcal{F}|}\}$, and
- c_l is the capacity of link l , for all $l \in \mathcal{L}$.

Each flow f traverses a subset of links $\mathcal{L}_f \subset \mathcal{L}$ and, similarly, each link l is traversed by a subset of flows $\mathcal{F}_l \subset \mathcal{F}$. Finally, each flow f transmits data at a rate r_f and the capacity constraint $\sum_{f \in \mathcal{F}_l} r_f \leq c_l$ must hold for all $l \in \mathcal{L}$.

A core concept upon which our mathematical framework rests is the notion of a *bottleneck link*. Intuitively, a flow is bottlenecked at a link if bypassing the link would allow its

transmission rate to increase. A link whose capacity is fully utilized is always a bottleneck of at least one flow, though not necessarily of all the flows traversing it. In this work, we adopt the following formal definition:

Definition 2. Bottleneck link. Let $\mathcal{N} = \langle \mathcal{L}, \mathcal{F}, \{c_l, \forall l \in \mathcal{L}\} \rangle$ be a network where each flow $f \in \mathcal{F}$ transmits data at a rate r_f as determined by a congestion control algorithm (e.g., TCP’s algorithm [1]). We will say that flow f is bottlenecked at link l —equivalently, that link l is a bottleneck of flow f —if and only if:

- Flow f traverses link l .
- $\partial r_f / \partial c_l^- \neq 0$. That is, the transmission rate of flow f changes upon small reductions in link l ’s capacity.¹

This characterization of bottlenecks is a generalization of some of the classic definitions found in the literature. Unlike previous work, however, it is based on the notion of a *perturbation*, mathematically expressed as a derivative of a flow rate with respect to the capacity of a link ($\partial r_f / \partial c_l$). As an example to illustrate that our definition of bottleneck is relatively loose, in Appendix A we show that it generalizes the classic max-min definition of Bertsekas and Gallager [8]. The generality of the definition of bottlenecks used in this paper suggests that our framework can be applied to a wide variety of rate allocation schemes—not only to max-min fairness [8], proportional fairness [9] and specific algorithms (e.g., BBR [2], Cubic [7], Reno [10], etc.), but to other classes of congestion control solutions that meet the conditions of Definition 2. We leave this promising direction for future work, and focus on the classic max-min setting considered in [3].

We complete the description of our network model by defining the concept of a link’s *fair share*:

Definition 3. Fair share of a link. Let $\mathcal{N} = \langle \mathcal{L}, \mathcal{F}, \{c_l, \forall l \in \mathcal{L}\} \rangle$ be a network. The *fair share* s_l of a link $l \in \mathcal{L}$ is the rate of the flows that are bottlenecked at link l .

As we will see throughout this work, the concept of link fair share is dual to the concept of flow rate, in that many of the mathematical properties that are applicable to the rate of a flow are also applicable to the fair share of a link.

2.2. The Gradient Graph

Our objective is to derive a mathematical framework capable not just of detecting but also of quantifying the influences that links and flows exert on each other. In [3], the authors introduced two bottleneck structures, the bottleneck precedence graph (BPG) and the gradient graph, and demonstrated that data networks qualitatively operate according to the BPG structure. The authors briefly described the concept of the gradient graph, but their work focused mostly on the mathematical properties of the bottleneck precedence

1. We use the notation $\partial y / \partial x^-$ to denote the left derivative. This subtlety is necessary because a flow can have multiple bottleneck links. In this case, decreasing the capacity of only one bottleneck would affect the rate of the flow, while increasing its capacity would not; thus, the (two-sided) derivative would not exist.

graph. In our paper, we instead focus on a modified version of the gradient graph structure. Our work stems from the insight that, as we will show, this structure enables not just qualitative analysis, as in [3], but also quantitative analysis, providing a framework to better understand and optimize network performance.

We start with the definition of the gradient graph:

Definition 4. *Gradient graph.* Let $\mathcal{N} = \langle \mathcal{L}, \mathcal{F}, \{c_l, \forall l \in \mathcal{L}\} \rangle$ be a network. The *gradient graph* is a directed graph such that:

- 1) There exists a vertex for each bottleneck link and each flow in the network.
- 2) For every flow $f \in \mathcal{F}$:
 - a) If f is bottlenecked at link $l \in \mathcal{L}$, then there exists a directed edge from l to f ;
 - b) If f traverses link $l \in \mathcal{L}$, then there exists a directed edge from f to l ;

For ease of exposition, in this paper we will use the terms gradient graph and bottleneck structure interchangeably. This definition is borrowed from [3], except for a subtle but relevant modification of 2b. (The rest of the theoretical developments presented in this work are new contributions.) Previously, edges were only included from flows to links that they traverse, but that do not bottleneck them. In this work, we also include edges from flows to their bottleneck links. We call these “backward edges”, and we introduce them because they are required by several of our theorems and algorithms.

The utility of our definition of gradient graph as a data structure for understanding network performance is captured in the following theorem:

Theorem 1. *Propagation of network perturbations.* Let $x, y \in \mathcal{L} \cup \mathcal{F}$ be a pair of links or flows in the network. Then a perturbation in the capacity c_x (for $x \in \mathcal{L}$) or transmission rate r_x (for $x \in \mathcal{F}$) of x will affect the fair share s_y (for $y \in \mathcal{L}$) or transmission rate r_y (for $y \in \mathcal{F}$) of y if and only if there exists a directed path from x to y in the gradient graph.

Proof. See Appendix B. □

Intuitively, the gradient graph of a network describes how perturbations in link capacities and flow transmission rates propagate through the network. Imagine that flow f is bottlenecked at link l . From Definition 2, this necessarily implies that a perturbation in the capacity of link l will cause a change on the transmission rate of flow f , $\partial r_f / \partial c_l \neq 0$. This is reflected in the gradient graph by the presence of a directed edge from a link l to a flow f (Condition 2a in Definition 4). A change in the value of r_f , in turn, affects all the other links traversed by flow f . This is reflected by the directed edges from f to the links it traverses (Condition 2b). This basic process of (1) inducing a perturbation in a vertex (either in a link or a flow vertex) followed by (2) propagating the effects of the perturbation along the departing edges of the vertex creates a ripple effect in the bottleneck structure

as described in Theorem 1. Leveraging this result, we can formally introduce the concept of *region of influence*:

Definition 5. *Regions of influence in a network.* The region of influence of a link or flow $x \in \mathcal{L} \cup \mathcal{F}$, denoted $\mathcal{R}(x)$, is the set of links and flows y that are reachable from x in the gradient graph.

The region of influence is an important concept in network performance analysis and optimization because it describes what parts of a network are affected by perturbations in the performance of a link or a flow. In Section 2.3, we will also see how such influences can be quantified.

We now introduce the *GradientGraph()* algorithm (Algorithm 1), a procedure that constructs the gradient graph of a network. The algorithm begins with crude estimates of the fair share rates of the links, and iteratively refines them until all the capacity in the network has been allocated and the rate of each flow reaches its final value. In the process, the gradient graph is constructed level by level. The algorithm starts by initializing the available capacity of each link (line 3), estimating its fair share (line 4) and adding all links to a min-heap by taking their fair share value as the key (line 5). At each iteration, the algorithm picks the unresolved link with the lowest fair share value from the min-heap (line 8). Once this link is selected, all unresolved flows remaining in the network that traverse it are resolved. That is, their rates are set to the fair share of the link (line 12) and they are added to the set of vertices of the gradient graph \mathcal{V} (line 13). In addition, directed edges are added in the gradient graph between the link and all the flows bottlenecked at it (line 10) and from each of these flows to the other links that they traverse (line 15). Lines 16-17-18 update the available capacity of the link, its fair share, and the position of the link in the min-heap according to the new fair share. Finally, the link itself is also added as a vertex in the gradient graph (line 22). This iterative process is repeated until all flows have been added as vertices in the gradient graph (line 7). The algorithm returns the gradient graph \mathcal{G} , the fair share of each link $\{s_l, \forall l \in \mathcal{L}\}$ and the rate of each flow $\{r_f, \forall f \in \mathcal{F}\}$.

We conclude this section stating the time complexity of the *GradientGraph()* algorithm:

Lemma 1. *Time complexity of GradientGraph().* The time complexity of running *GradientGraph()* is $O(|\mathcal{L}| \log |\mathcal{L}| \cdot H)$, where H is the maximum number of flows that traverse a single link.

Proof. See Appendix E. □

2.3. Link and Flow Gradients

In this section, we focus on the problem of quantifying the ripple effects created by perturbations in a network. Because networks are composed of links and flows, there are two kinds of perturbations: (1) those originating from changes to the capacity of a link and (2) those originating from changes to the rate of a flow. When such changes occur, the congestion control algorithm adjusts its allocation

Algorithm 1 GradientGraph($\mathcal{N} = \langle \mathcal{L}, \mathcal{F}, \{c_l, \forall l \in \mathcal{L}\} \rangle$)

```
1:  $\mathcal{V} = \emptyset; E = \emptyset; r_f = \infty, \forall f \in \mathcal{F};$ 
2: for  $l \in \mathcal{L}$  do
3:    $a_l = c_l;$  # available capacity
4:    $s_l = a_l / |\mathcal{F}_l|;$  # fair share
5:   MinHeapAdd(key =  $s_l$ , value =  $l$ );
6: end for
7: while  $\mathcal{F} \not\subseteq \mathcal{V}$  do
8:    $l = \text{MinHeapPop}();$ 
9:   for  $f \in \mathcal{F}_l$  such that  $r_f \geq s_l$  do
10:     $E = E \cup \{(l, f), (f, l)\};$ 
11:    if  $f \notin \mathcal{V}$  then
12:       $r_f = s_l;$ 
13:       $\mathcal{V} = \mathcal{V} \cup \{f\};$ 
14:      for  $l' \in \mathcal{L}_f$  such that  $r_f < s_{l'}$  do
15:         $E = E \cup \{(f, l')\};$ 
16:         $a_{l'} = a_{l'} - s_l$ 
17:         $s_{l'} = a_{l'} / |\mathcal{F}_{l'} \setminus \mathcal{V}|;$ 
18:        MinHeapUpdateKey(value =  $l'$ , newKey =  $s_{l'}$ );
19:      end for
20:    end if
21:  end for
22:   $\mathcal{V} = \mathcal{V} \cup \{l\};$ 
23: end while
24: return  $\langle \mathcal{G} = \langle V, E \rangle, \{s_l, \forall l \in \mathcal{L}\}, \{r_f, \forall f \in \mathcal{F}\} \rangle;$ 
```

of bandwidth to the flows so as to maintain two objectives: (1) maximizing network utilization while (2) ensuring fairness among competing flows. The congestion control algorithm acts like a function mapping network conditions (including its topology, link capacities, and flow paths) to rate allocations. Large changes in any of these inputs can have complicated ripple effects on the flow rates, but for sufficiently small changes, the bandwidth allocation function is linear.² This local linearity property naturally motivates the concept of link and flow gradients:

Definition 6. *Link and flow gradients.* Let $\mathcal{N} = \langle \mathcal{L}, \mathcal{F}, \{c_l, \forall l \in \mathcal{L}\} \rangle$ be a network. We define:

- The *gradient* of a link $l \in \mathcal{L}$ with respect to another link $l^* \in \mathcal{L}$ as $\nabla_{l^*}(l) = \partial s_l / \partial c_{l^*}$;
- The *gradient* of a flow $f \in \mathcal{F}$ with respect to some link $l^* \in \mathcal{L}$ as $\nabla_{l^*}(f) = \partial r_f / \partial c_{l^*}$;
- The *gradient* of a link $l \in \mathcal{L}$ with respect to a flow $f^* \in \mathcal{F}$ as $\nabla_{f^*}(l) = \partial s_l / \partial r_{f^*}$;
- The *gradient* of a flow $f \in \mathcal{F}$ with respect to another flow $f^* \in \mathcal{F}$ as $\nabla_{f^*}(f) = \partial r_f / \partial r_{f^*}$.

Intuitively, the gradient with respect to a link measures the impact that a small perturbation in its capacity has on another link or flow. In real networks, this corresponds to the scenario of physically upgrading a link or, in programmable networks (e.g., [11]), logically modifying the capacity of a virtual link. Thus, link gradients can generally be used to resolve network design and capacity planning problems. Similarly, the gradient with respect to a flow measures the impact that a perturbation in its rate has on a link or another flow. This scenario corresponds, for instance, to the case of traffic shaping a flow to alter its transmission rate or changing the route of a flow—which can be seen as dropping

2. Technically, it is piecewise linear, like the absolute value function, so picking a linear function that locally approximates it requires knowing the direction of the change.

the rate of that flow down to zero and adding a new flow with a different path. Thus, flow gradients can generally be used to resolve traffic engineering problems. In Section 3 we will see applications in real networks that illustrate each of these scenarios.

We now present an algorithm called *ForwardGrad()* (Algorithm 2) for calculating link and flow gradients. The algorithm takes a set of links and flows, the gradient graph of the corresponding network, a link or flow x with respect to which to compute the gradients, and a direction Δx of the perturbation. It outputs the gradients of all links and flows in the network with respect to x . *ForwardGrad()* takes inspiration from forward mode automatic differentiation (“Forward Prop”) [12], an algorithm that uses directed acyclic graphs to represent complicated mathematical functions as compositions of simpler functions, whose derivatives can be composed by repeatedly applying the chain rule. In the case of congestion control, we do not have a closed-form mathematical formula that relates network conditions (the inputs) to the flow rates and fair share values (the outputs), but we can use the gradient graph to break down and optimize this function.

The thrust of the algorithm is as follows. For all $l \in \mathcal{L}$, let Δ_l be the change in the fair share rate of link l . For all $f \in \mathcal{F}$, let Δ_f be the change in the rate of flow f . We call these variables the “drifts” caused by a perturbation. Before the perturbation, $\Delta_l = \Delta_f = 0$ for all links and flows. To begin the algorithm, we make an infinitesimally small perturbation in the independent variable (the one in the “denominator” of the derivative) that can be positive or negative. If the independent variable x is a flow f , we set $\Delta_f = \delta$ (line 2). If it is a link l , and S_l is the set of direct successors of node l in the gradient graph, we set $\Delta_l = \delta / |S_l|$ (line 3). This is done since, by definition of the gradient graph, $|S_l|$ is the number of flows bottlenecked at l and the change in l ’s capacity will be distributed evenly among these flows. To determine how this perturbation propagates to the rest of the network, we follow all directed paths from that vertex and update the drifts according to the following two invariants:

- *Invariant 1: Flow Equation.* A flow’s drift Δ_f equals the minimum drift of its bottleneck links. That is, $\Delta_f = \min_{l \in P_f} \Delta_l$, where P_f is the set of links visited directly before flow vertex f on a path from the starting vertex x (the predecessors in the graph).
- *Invariant 2: Link Equation.* A link’s drift Δ_l is the negative of the flow drifts entering its vertex, divided by the number of flow drifts leaving it. That is, $\Delta_l = -\sum_{f \in P_l} \Delta_f / |S_l|$, where P_l is the set of flow vertices visited directly before link vertex l and S_l is the set of flow vertices visited directly after link vertex l on a path from the starting vertex x .

Finally, the derivative of a given variable with respect to the independent variable that we perturbed can be calculated by dividing its drift by δ . In particular, assume the capacity of link l is the independent variable that we perturbed and let the rate of flow f be the dependent variable in which

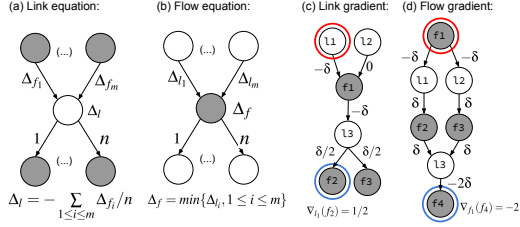


Figure 1: (a) Link equation, (b) flow equation, and examples of (c) link gradient and (d) flow gradient.

we want to measure the effect of this perturbation. Then, $\partial r_f / \partial c_l = \Delta_f / \delta$.

Since the flow and link equations lie at the heart of the algorithm, we provide some further explanation. Invariant 1 ensures that the capacity limits are respected and the network's resources are not wasted. Each flow must use exactly the amount of bandwidth allocated by its bottleneck link, so if the bottleneck's fair share changes, the flow's rate must change too. It also ensures fairness, since each flow bottlenecked at a certain link will experience the same drift. Invariant 2 ensures that capacity is neither created nor destroyed through the process of propagating a perturbation, except at the link whose capacity was initially perturbed. If a link's predecessors are using less bandwidth than before, then the savings must be redistributed evenly among the other flows that traverse the link.

Fig. 1(a) and (b) show graphical representations of the link and flow equations. Fig. 1(c) and (d) present two simple examples of gradient graphs that we use to illustrate how to compute link and flow gradients. Note that throughout the paper, we use white vertices to denote bottleneck links and gray vertices to denote flows. We also omit backward edges for visual simplicity. Fig. 1(c) presents the case of computing the link gradient $\nabla_{l_1}(f_2)$. A perturbation is applied to link l_1 that decreases its capacity c_{l_1} by an infinitesimally small amount δ . Since only one flow is bottlenecked at l_1 , we have $\Delta_{l_1} = -\delta$. This perturbation propagates to flow f_1 according to the flow equation: $\Delta_{f_1} = \min\{\Delta_{l_1}, \Delta_{l_2}\} = \min\{-\delta, 0\} = -\delta$. The perturbation is propagated down to link l_3 according to the link equation: $\Delta_{l_3} = -\Delta_{f_1}/2 = \delta/2$. Finally, applying the flow equation for f_2 , we obtain the flow drift $\Delta_{f_2} = \delta/2$. Thus, the gradient of flow f_2 with respect to link l_1 is $\nabla_{l_1}(f_2) = \Delta_{f_2}/\delta = 1/2$. Fig. 1d illustrates a simple example of flow gradient computation. We leave it to the reader to verify that, for this bottleneck structure, the gradient of flow f_4 with respect to flow f_1 is $\nabla_{f_1}(f_4) = -2$.

To make this process into a precise algorithm, we still must specify the order in which to process the vertices of the graph. At each step, the vertex we process must be a neighbor of one of the vertices we have already visited. Even though backward edges create loops in the gradient graph, we never visit a vertex twice. If multiple vertices meet these criteria, we pick the one with the minimal rate or fair share value. If there are multiple vertices with the minimal rate or fair share value, we pick the one that would receive the

minimum drift if it were processed next (see line 15 where keys in the heap are ordered pairs of rate/fair share and drift). This reflects the order in which the bottleneck structures are constructed in Algorithm 1, which itself reflects the order in which the rates and fair shares converge in congestion controlled networks [3]. That is, we first visit the vertex that would receive the smallest rate or fair share if the perturbation were applied and bandwidth were reallocated from scratch. This completes the description of the *ForwardGrad()* algorithm.

Algorithm 2 ForwardGrad($\mathcal{L}, \mathcal{F}, \mathcal{G}, x \in \mathcal{L} \cup \mathcal{F}, \Delta x \in \{\pm 1\}$)

```

1:  $\Delta c_l = 0 \quad \forall l \in \mathcal{L}$ 
2:  $\Delta r_f = 0 \quad \forall f \in \mathcal{F}$  # Drift of flow  $f$ 
3:  $\Delta s_l = 0 \quad \forall l \in \mathcal{L}$  # Drift of link  $l$ 
4: if  $x \in \mathcal{F}$  then
5:    $\Delta u_x = \Delta x$ 
6:   MinHeapAdd(key =  $\langle u_x, \Delta u_x \rangle$ , value =  $x$ )
7: else if  $x \in \mathcal{L}$  then
8:    $\Delta c_x = \Delta x$ 
9:    $\Delta s_x = \Delta c_x / |\text{successors}(x, \mathcal{G})|$ 
10:  MinHeapAdd(key =  $\langle s_x, \Delta s_x \rangle$ , value =  $x$ )
11: end if
12:  $V = \emptyset$  # the set of previously visited nodes
13: repeat
14:   repeat
15:      $y = \text{MinHeapPop}()$ ; # Get the next unvisited node
16:   until  $y \notin \emptyset$ 
17:    $V = V \cup \{y\}$ 
18:   if ( $y \in \mathcal{L}$  and  $\Delta s_y = 0$ ) or ( $y \in \mathcal{F}$  and  $\Delta u_y = 0$ ) then
19:     Continue
20:   end if
21:   for  $y' \in \text{successors}(y, \mathcal{G}) \setminus V$  do
22:     if  $y' \in \mathcal{F}$  then
23:        $\Delta r_{y'} = \min_{l \in \pi(y', \mathcal{G})} \Delta s_l$  # Flow equation invariant
24:       MinHeapAdd(key =  $\langle r_{y'}, \Delta r_{y'} \rangle$ , value =  $y'$ )
25:     else if  $y' \in \mathcal{L}$  then
26:        $\Delta c_{y'} = \Delta c_{y'} - \Delta u_{y'}$ 
27:        $\Delta s_{y'} = \Delta c_{y'} / |\text{successors}(y', \mathcal{G}) \setminus V|$  # Link equation invariant
28:       MinHeapAdd(key =  $\langle s_{y'}, \Delta s_{y'} \rangle$ , value =  $y'$ )
29:     end if
30:   end for
31: until MinHeapEmpty()
32: return  $\langle \Delta s_l \quad \forall l \in \mathcal{L}, \Delta r_f \quad \forall f \in \mathcal{F} \rangle$ 

```

The next two theorems show that Algorithm 2 is both correct and efficient.

Theorem 2. *Correctness of ForwardGrad().* Let $\mathcal{N} = \langle \mathcal{L}, \mathcal{F}, \{c_l, \forall l \in \mathcal{L}\} \rangle$ be a network and let \mathcal{G} be the corresponding gradient graph. Let $x \in \mathcal{L} \cup \mathcal{F}$. After running Algorithm 2, $\Delta s_l = \nabla_x(l)$ for all $l \in \mathcal{L}$, and $\Delta r_f = \nabla_x(f)$ for all $f \in \mathcal{F}$.

Proof. See Appendix C. □

Theorem 3. *Time complexity of ForwardGrad().* Let $x \in \mathcal{L} \cup \mathcal{F}$. Then Algorithm 2 finds the gradients of all links and flows in the network with respect to x in time $O(|\mathcal{R}(x)| \cdot \log |\mathcal{R}(x)|)$.

Proof. See Appendix D. □

To conclude and complement this section, we state an upper bound on the value of the gradients:

Property 1. *Gradient bound.* Let $\mathcal{N} = \langle \mathcal{L}, \mathcal{F}, \{c_l, \forall l \in \mathcal{L}\} \rangle$ be a network and let \mathcal{G} be its gradient graph. Let δ be an

infinitesimally small perturbation performed on a flow or link $x \in \mathcal{L} \cup \mathcal{F}$, producing a drift Δ_y , for all $y \in \mathcal{L} \cup \mathcal{F}$. Then, $|\nabla_x(y)| = |\Delta_y|/\delta \leq d^{D(X)/4}$, where $D(X)$ is the diameter of a graph X and d is the maximum indegree and outdegree of any vertex in the graph.

Proof. See Appendix F. \square

3. Applications to Data Networks and Experimental Results

Because bottleneck structures are a fundamental property intrinsic to any congestion-controlled data network, its applications span a variety of networking problems. In this section, our goal is to present examples and experiments illustrating how QTBS can be used to resolve some of these problems. We will see that in each of them, the framework is able to provide new insights into one or more operational aspects of a network. The examples presented in this section are not exhaustive, but only illustrative. To help organize the applications, we divide them in two main classes: traffic engineering and capacity planning. For each of these classes, we provide specific examples of problems that relate to applications commonly found in modern production networks.

To experimentally demonstrate that data networks behave qualitatively and quantitatively according to QTBS, we use *Mininet-G2* [13], a network emulation framework developed by our team that consists of a set of software modules and extensions to Mininet [14]. Leveraging software define networking (SDN), *Mininet-G2* enables the creation and analysis of arbitrary network architectures using real production TCP/IP code, including production-grade implementations of congestion control algorithms such as BBR, Cubic or Reno. (See also Appendix G for more information.) We are open sourcing *Mininet-G2* and all the experiments presented in this paper, hoping this will also enable the research community to verify our findings and further experiment with the theory of bottleneck structures.

All the experimental results presented in this section are based on Google’s BBR congestion control algorithm [2]. Results for similar experiments using Cubic [7] can be found in Appendix G. For each experiment, we used Jain’s fairness index [15] as an estimator to measure how closely the predictions of the theory of bottleneck structure model match the experimental results. For all BBR experiments presented in the next sections, this index was above 0.99 accuracy on a scale from 0 to 1 (See Appendix G), reflecting the strength of QTBS in modeling network behavior.

3.1. Traffic Engineering: Computation of the Highest-Throughput Route

In traditional IP networks, the problems of flow routing and congestion control are separately resolved by following a two-step process: first, a routing protocol (e.g., BGP [16], OSPF, etc.) is used to determine the path between any two nodes in a network; then, flows are routed according to

such paths and their transmission rates are regulated using a congestion control algorithm (e.g., BBR [2]). This layered and disjoint approach is known to be scalable but suboptimal because the routing algorithm identifies paths without taking into account the flow transmission rates assigned by the congestion control algorithm [4], [17], [18], [19].

In this section, we use QTBS to resolve the following joint routing and congestion control problem in a scalable manner:

Definition 7. *Flow-rate maximal routing.* Let $\mathcal{N} = \langle \mathcal{L}, \mathcal{F}, \{c_l, \forall l \in \mathcal{L}\} \rangle$ be a network and suppose that a new flow f arrives. We will say that a routing algorithm is *flow-rate maximal* if it routes flow f through a path that maximizes its transmission rate r_f .

In traditional IP routing, all packets transmitted from a source to a destination node follow the same *lowest-cost* route [16]. This rigidity leads to the well-known fish problem [8], whereby certain paths in a network become congested while other paths are underutilized. A flow-rate maximal algorithm, instead, is able to bypass points of congestion by assigning new flows to the highest-throughput path available given the current usage of the network.

One might mistakenly think that the least congested path can be identified by looking for links with small fair shares (Definition 3). However, the placement of a new flow onto a given path will itself alter the state of the network, changing those fair shares and potentially rendering the chosen path sub-optimal. In this section, we show that QTBS can be used to identify the maximal-rate path for a flow while taking into account the perturbations created by the placement of the flow itself, thus solving the flow-rate maximal routing problem.

MaxRatePath() (Algorithm 3) is an algorithm that uses QTBS to compute flow-rate maximal paths. It takes the following inputs: a network $\mathcal{N} = \langle \mathcal{L}, \mathcal{F}, \{c_l, \forall l \in \mathcal{L}\} \rangle$, the set of routers \mathcal{U} , and the source and the destination routers of the flow we intend to route, u_s and u_d . By convention, a link $l \in \mathcal{L}$ is identified with the tuple $l = (u_x, u_y)$, where $u_x, u_y \in \mathcal{U}$ are the two routers connected by link l . The algorithm returns the new flow f , expressed as the set of links it traverses, guaranteeing they form a path from u_s to u_d that yields the maximal rate r_f for f .

As the pseudocode shows, *MaxRatePath()* is based on Dijkstra’s shortest path algorithm, with routers as vertices and links as edges in the network topology graph. The difference resides in the way the “distance” to a neighboring router u' is calculated (lines 12-14). In *MaxRatePath()*, this value represents not the number of hops on the shortest path from u_s to u' , but the inverse of the largest possible rate that a flow would experience if it were added on some path from u_s to u' . That is, the distance to u' is the smallest possible time needed to send 1 bit of information from u_s to u' . Unlike in the standard Dijkstra’s algorithm, this value cannot be computed by adding an edge length to d_u , the distance to a neighbor of u' . Instead, we create a new flow f by extending the optimal path from u_s to u . So at each iteration of the algorithm, f takes the path $u_s \rightarrow \dots \rightarrow u \rightarrow u'$

(line 12). We then construct the gradient graph that would correspond to this network if the new flow f were added (line 13). Finally, we use the inverse of the the rate assigned to the new flow r_f as the distance value (line 14). In the pseudocode, we invoke the *GradientGraph()* algorithm in line 13, reconstructing the gradient graph from scratch to include the new flow. However, we can get this result more efficiently by updating the initial gradient graph (the one corresponding to the network before adding the new flow), since the new flow will only affect a subset of the existing links and flows. We leave the precise algorithm for performing this update to future work.

Algorithm 3 MaxRatePath($\mathcal{N} = \langle \mathcal{L}, \mathcal{F}, \{c_l, \forall l \in \mathcal{L}\} \rangle, \mathcal{U}, u_s \in \mathcal{U}, u_d \in \mathcal{U}$)

```

1: F = MinHeap(); # Frontier set
2: C = Set(); # Converged set
3:  $d_u = \infty, \forall u \in \mathcal{U}$ ; # Initialize distance metric
4:  $d_{u_s} = 0$ ;
5: F.insert(key = 0, value =  $u_s$ );
6: while  $u = F.extractMin()$  do
7:   C.insert( $u$ ); # Has converged
8:   if  $u == u_d$  then
9:     break;
10:  end if
11:  for all  $(u, u') \in \mathcal{L}$  and  $u' \notin C$  do
12:     $f = \{(x_1, x_2), (x_2, x_3), \dots, (x_{i-1}, x_i) \mid x_j \in C, (x_j, x_{j+1}) \in \mathcal{L}, x_1 = u_s, x_{i-1} = u, x_i = u'\}$ ;
13:     $\langle \mathcal{G}, \{s_l\}, \{r_f\} \rangle = \text{GradientGraph}(\mathcal{N} = \langle \mathcal{L}, \mathcal{F} \cup \{f\}, \{c_l, \forall l \in \mathcal{L}\} \rangle)$ ;
14:     $distance = 1/r_f$ ; # Flow completion time to send 1 bit
15:    if  $d_{u'} \leq distance$  then
16:      continue;
17:    end if
18:     $d_{u'} = distance$ ;
19:    if  $u' \notin F$  then
20:      F.insert(key =  $d_{u'}$ , value =  $u'$ );
21:    else
22:      F.update(key =  $d_{u'}$ , value =  $u'$ );
23:    end if
24:  end for
25: end while
26:  $f = \{(x_1, x_2), (x_2, x_3), \dots, (x_{i-1}, x_i) \mid x_j \in C, (x_j, x_{j+1}) \in \mathcal{L}, x_1 = u_s, x_i = u_d\}$ ;
27: return  $f$ ;

```

Lemma 2. Correctness of the MaxRatePath algorithm. Let $\mathcal{N} = \langle \mathcal{L}, \mathcal{F}, \{c_l, \forall l \in \mathcal{L}\} \rangle$ be a network and \mathcal{U} the set of its routers. Suppose that f and f' are two flows not in \mathcal{F} that originate at router u_s and end at router u_d . Then $f = \text{MaxRatePath}(\mathcal{N}, \mathcal{U}, u_s, u_d)$ implies $r_f \geq r_{f'}$.

Proof. The proof of this lemma is constructive and describes a procedure to efficiently compute the maximal-rate path of a flow using the bottleneck structure. See Appendix G for details. \square

To illustrate how we can use QTBS and the MaxRatePath algorithm to compute the highest-throughput path for a given flow, consider the network shown in Fig. 2a. This topology corresponds to Google’s B4 network as described in [20], the SDN-WAN network that connects Google’s data centers globally. For the sake of illustration, we will assume there are two flows (one for each direction) connecting every data center in the US with every data

center in Europe, with all flows routed along a shortest path from source to destination. Since there are six data centers in the US and four in Europe, this configuration has a total of 48 flows ($|\mathcal{F}| = 6 \times 4 \times 2 = 48$). (See Table 7 in Appendix G for a description of the exact path followed by each flow.) All links are assumed to have a capacity of 10 Gbps except for the transatlantic links, which are configured at 25 Gbps (i.e., $c_l = 10$, for all $l \notin \{l_8, l_{10}\}$, $c_{l_8} = c_{l_{10}} = 25$). While obviously production networks operate with a much higher number of flows, in our example we use a reduced number to simplify the descriptions of the bottleneck structures and the steps followed to resolve the given problem. This simplification is without loss of generality, and the same approach is applicable to large scale operational networks. (See Appendix G for notes on integration with production networks.)

Fig. 2b shows the corresponding bottleneck structure obtained from running Algorithm 1 on the proposed network configuration. This structure shows that flows are organized in two levels: the top-level includes flows $\{f_1, f_2, f_3, f_4, f_5, f_7, f_8, f_{10}, f_{13}, f_{14}, f_{15}, f_{16}\}$ and the low-level includes flows $\{f_6, f_9, f_{11}, f_{12}, f_{17}, f_{18}, f_{19}, f_{20}, f_{21}, f_{22}, f_{23}, f_{24}\}$. Note that because each pair of data centers is connected via two flows (one for each direction), without loss of generality, in Fig. 2b we only include the first 24 flows (flows transferring data from US to Europe), since the results are symmetric for rest of the flows—i.e., flow f_i has the same theoretical transmission rate and is positioned at the same level in the bottleneck structure as flow f_{i+24} for all $1 \leq i \leq 24$. Note also that all the top-level flows operate at a lower transmission rate (with all rates at 1.667) than the bottom-level flows (with rates between 2.143 and 3). As was proven in [3], this is in fact a property of all bottleneck structures: flows operating at lower levels of the bottleneck structure have greater transmission rates than those operating at higher levels.

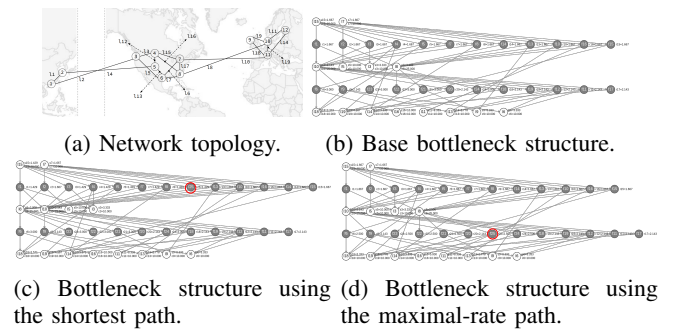


Figure 2: Computation of maximal-throughput path for flow f_{25} .

Under this configuration, suppose that we need to initiate a new flow f_{25} to transfer a large data set between data centers 4 and 11. For instance, this flow could correspond to the transmission of a terabyte data set from a data center in the US to another in Europe. Our objective in this exercise is to identify a high-throughput route to minimize the time required to transfer the data.

In Fig. 2c we show the bottleneck structure obtained for the case that f_{25} uses the shortest path $l_{15} \rightarrow l_{10}$. For instance, this corresponds to the solution obtained from running BGP [16] with a link cost metric equal to 1. Using this path, the new flow would be placed at the upper bottleneck level—i.e., the lower-throughput level—in the bottleneck structure, receiving a theoretical rate of $r_{25} = 1.429$. Note that the presence of this new flow slightly modifies the performance of some of the flows on the first level (flows $\{f_1, f_3, f_4, f_5, f_7, f_8\}$ experience a rate reduction from 1.667 to 1.429), but it does not modify the performance of the flows operating at the bottom level. This is because, for the given configuration, the new flow only creates a shift in the distribution of bandwidth on the top level, but the total amount of bandwidth used in this level stays constant. (In Fig. 2b, the sum of all the flow rates on the top bottleneck level is $1.667 \times 12 = 20$, and in Fig. 2c this value is the same: $1.429 \times 7 + 1.667 \times 6 = 20$.) As a result, the ripple effects produced from adding flow f_{25} into the network cancel each other out without propagating to the bottom level.

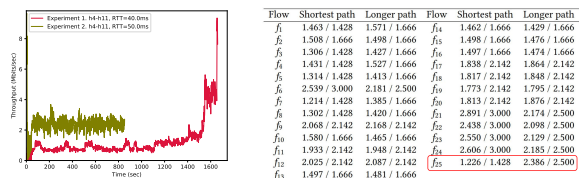
While $l_{15} \rightarrow l_{10}$ is the shortest path, it is not the path with the highest throughput. To find such a path, we run the MaxRatePath procedure (Algorithm 3) and obtain the solution $l_{16} \rightarrow l_8 \rightarrow l_{19}$. The resulting bottleneck structure is shown in Fig. 2d. Using this path, flow f_{25} would now be placed at the bottom level—the higher-throughput level—in the bottleneck structure, thus resulting in a rate value $r_{25} = 2.5$, an increase of 74.95% with respect to the shortest path solution. Another positive outcome of this solution is that none of the flows operating at the upper level (the flows that receive less bandwidth) see their rate reduced. This is a direct consequence of Theorem 1, since a perturbation on lower levels can have no ripple effects on upper levels. It constitutes also a natural fairness property of the MaxRatePath algorithm: as the procedure assigns maximal-throughput paths to new incoming flows, such flows tend to be placed at the bottom of the bottleneck structure (where the high-throughput links are located), thus tending to create no negative impact on the lower-throughput flows located at the top of the structure.

In the remainder of this section, we set out to empirically confirm these results. We start by creating the B4 network configuration shown in Fig. 2a using *Mininet-G2*. Following our example, we deploy a total of 48 shortest-path flows connecting every pair of nodes (in both directions) between the US and Europe. (Table 7 in Appendix G presents the exact path followed by each flow.) We then add two extra flows labeled f_{25} and f_{50} (one for each direction) to connect data centers 4 and 11 and perform two separate experiments: one placing the flows on the shortest path $l_{15} \leftrightarrow l_{10}$ and another one placing them on the longer path $l_{16} \leftrightarrow l_8 \leftrightarrow l_{19}$.

Fig. 3a shows the rate of flow f_{25} for the two experiments (very similar results are obtained for the reverse-path flow f_{50} , see Appendix G). In the legend of this plot, experiment 1 and 2 correspond to the shortest and the (longer) maximal-throughput path configurations, respectively. As predicted by the bottleneck structure, the longer

path achieves a higher throughput and, thus, a lower flow completion time. Fig. 3b presents the average throughput obtained for all twenty-five flows from the US to Europe and for each of the two experiments, alongside the theoretical values according to the bottleneck structure. (The results obtained from the other twenty-five flows on the reverse path are similar and can be found in Appendix G.) As shown, flow f_{25} achieves a performance of 1.226 and 2.386 Mbps for the shortest and longer paths, respectively—with the theoretical rates being 1.428 and 2.5 Mbps, respectively. Thus, the longer path yields a 94% improvement on flow throughput compared to the shortest path. For all the experiments run in this section, Jain’s fairness index was above 0.99 (see Appendix G), indicating the accuracy of QTBS in predicting flow performance.

This experiment illustrates that using QTBS, it is possible to identify routes that are highly efficient from a congestion control standpoint. Note that this contrasts with traditional approaches that perform traffic engineering by separating the routing and congestion control problems, so that the routing algorithm is unaware of the choices made by the congestion control algorithm and vice versa. See for instance Section 5.3.1 in [4], which discusses the potential advantages of performing joint routing and congestion control in Google’s WAN, but leaves this direction as future work. We reason that QTBS provides a mathematical framework to connect both problems, identifying routes that are globally efficient from both a topological and a congestion control standpoints.



(a) Acceleration of flow f_{25} . (b) Experimental vs theoretical flow rates (Mbps).

Figure 3: Identification of a high-bandwidth route to accelerate the performance of flow f_{25} .

3.2. Capacity Planning: Design of Optimal Fat-Tree Networks in Data Centers

As Leiserson demonstrated in his seminal paper [6], fat-trees are universally efficient networks in the following sense: for a given network size s , a fat-tree can emulate any other network that can be laid out in that size s with a performance slowdown at most logarithmic in s . This property makes fat-tree topologies highly competitive and is one of the reasons they are so widely used in large-scale data centers [5] and high-performance computing (HPC) networks [21]³. In this experiment, we use QTBS

3. In the context of data centers, fat-tree networks are also known as folded-clos or spine-and-leaf networks [5].

to demonstrate that, due to the effects of the congestion control algorithm, there exists an optimal trade-off in the allocation of capacity at the top levels of the fat-tree. Further, we show that the optimal bandwidth allocation on the top level deviates from commonly accepted best practices in the design of full fat-tree networks that tend to equate the amount of bandwidth going up and down the tree at each switch [22].

Consider the network topology in Fig. 4a, which corresponds to a binary fat-tree with three levels and six links ($\mathcal{L} = \{l_1, l_2, \dots, l_6\}$). Assume also that there are two flows (one for each direction) connecting every pair of leaves in the fat-tree network, providing bidirectional full-mesh connectivity among the leaves. Since there are four leaves, that's a total of $4 \times 3 \times 2 = 24$ flows. All of the flows are routed following the shortest path. (See Table 8 in Appendix G for a description of the exact path followed by each flow.) For the sake of convention, we will adopt the terminology from data center architectures and use the names *spine* and *leaf* links to refer to the upper and lower links of the fat-tree network, respectively [5].

We fix the capacity of the leaf links to a value λ (i.e., $c_{l_1} = c_{l_2} = c_{l_3} = c_{l_4} = \lambda$) and the capacity of the spine links to $\lambda \times \tau$ (i.e., $c_{l_5} = c_{l_6} = \lambda \times \tau$), where τ is used as a design parameter enabling a variety of network configurations. For instance, in our binary fat-tree example, the case $\tau = 2$ corresponds to a full fat-tree network [22], because the total aggregate bandwidth at each level of the tree is constant, $c_{l_1} + c_{l_2} + c_{l_3} + c_{l_4} = c_{l_5} + c_{l_6} = 4\lambda$. Similarly, the case $\tau = 1$ corresponds to a thin-tree network, since it results with all the links having the same capacity, $c_{l_i} = \lambda$, for all $1 \leq i \leq 6$. The technique of optimizing the performance-cost trade-off of a fat-tree network by adjusting the capacity of the spine links is sometimes known as *bandwidth tapering* [21], [23]. The focus of our experiment is to use the bottleneck structure analysis to identify optimized choices for the tapering parameter τ .

In Fig. 4 we present a sequence of bottleneck structures (obtained from running Algorithm 1) corresponding to our fat-tree network with three different values of the tapering parameter τ and fixing $\lambda = 20$. (Note that the fixing of λ to this value is without loss of generality, as the following analysis applies to any arbitrary value $\lambda > 0$.) The first bottleneck structure (Fig. 4b) corresponds to the case $\tau = 1$ (i.e., all links have the same capacity, $c_{l_i} = 20$, for all $1 \leq i \leq 6$), which has all flows confined in one of two possible levels: a top level, where flows perform at a lower rate, $r_{f_2} = r_{f_3} = r_{f_5} = r_{f_6} = r_{f_7} = r_{f_8} = r_{f_{10}} = r_{f_{11}} = 2.5$; and a bottom level, where flows perform at twice the rate of the top-level flows, $r_{f_1} = r_{f_4} = r_{f_9} = r_{f_{12}} = 5$. This configuration is thus unfair to those flows operating at the top bottleneck, which receive half the bandwidth of the flows at the bottom level. Furthermore, this configuration is also inefficient at supporting applications with symmetric workload patterns—where all nodes approximately send the same amount of bytes to each other—because the completion time of the slowest flows is significantly higher (twice as high since they get half the rate) than the faster flows. Let us

next consider how we can use QTBS to identify a value of τ that minimizes the maximum completion time of any of the flows under the assumption of symmetric workloads.

By looking at the bottleneck structure in Fig. 4b, we see that the slowest flows are confined in the top bottleneck level. In order to increase the rates of these flows, we need to increase the tapering parameter τ that controls the capacity of the spine links l_5 and l_6 . This change transforms the bottleneck structure by bringing the two levels closer together, until, for a large enough value of τ , they fold. We can find this collision point using the link gradients as follows. Using *ForwardGrad()* (Algorithm 2), we obtain a link gradient value of $\nabla_l(f) = 0.125$ for all spine links $l \in \{l_5, l_6\}$ and top-level flows $f \in \{f_2, f_3, f_5, f_6, f_7, f_8, f_{10}, f_{11}\}$. On the other hand, the link gradient of any of the *low*-level flows with respect to any of the spine links is $\nabla_l(f) = -0.25$, for all $l \in \{l_5, l_6\}$ and $f \in \{f_1, f_4, f_9, f_{12}\}$. That is, an increase by one unit on the capacity of the spine links increases the rate of the top-level flows by 0.125 and decreases the rate of the low-level flows by 0.25. Since the rates of the top and low-level flows are 2.5 and 5, respectively, this means that the two levels will fold at a point where the tapering parameter satisfies the equation $2.5 + 0.125 \cdot \tau \cdot \lambda = 5 - 0.25 \cdot \tau \cdot \lambda$, yielding $\tau = 4/3$ and $c_{l_5} = c_{l_6} = 26.667$. The resulting bottleneck structure for this configuration is shown in Fig. 4c, confirming the folding of the two levels. This fat-tree configuration is optimal in that the flow completion time of the slowest flow is minimal. Because the bottleneck structure is folded into a single level, this configuration also ensures that all flows perform at the same rate, $r_{f_i} = 3.333$, for all $1 \leq i \leq 6$.

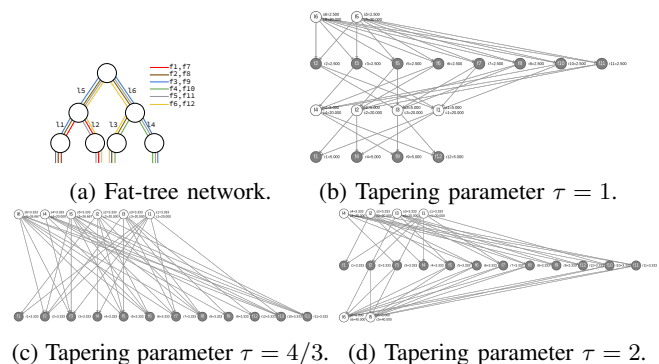


Figure 4: Design of optimal 3-level binary fat-trees.

What is the effect of increasing the tapering parameter above $4/3$? This result is shown in Fig. 4d for the case of a full fat-tree $\tau = 2$, i.e., $c_{l_5} = c_{l_6} = 40$. In this case, the two spine links are no longer bottlenecks to any of the flows (since these links are leaves in the bottleneck structure), but all flows continue to perform at the same rate, $r_{f_i} = 3.333$, for all $1 \leq i \leq 6$. Thus, increasing the capacity of the upper-level links above 26.667 does not yield any benefit, but increases the cost of the network. This result indicates that the fat-tree network shown in Fig. 4a should not be designed with an allocation of capacity on the spine links

higher than $\tau = 4/3$ times the capacity of the leaf links. In summary, we have that:

- A tapering parameter $\tau \geq 4/3$ should not be used, since the resulting network is just as efficient as a design with $\tau = 4/3$, but more costly.
- A tapering parameter $\tau = 4/3$ is optimal in that it minimizes the flow completion time of the slowest flow. This should be the preferred design in symmetric workloads that transfer about the same amount of data between all pairs of nodes.
- A tapering parameter $\tau < 4/3$ can be used if workloads are asymmetric, identifying the right value of τ that produces the right amount of bandwidth at each level of the bottleneck structure according to the workload.

In the rest of this section, we empirically demonstrate the existence of an optimal fat-tree design at $\tau = 4/3$ using Mininet-G2 [13] configured with the congestion control algorithm BBR. Fig. 5 presents the results of the experiments for the three values of the tapering parameter, $\tau \in \{1, 4/3, 2\}$. Each plot shows the transmission rate of all twelve flows as part of the network configuration, with each flow transmitting a total of 64 MB of data. Following the example in Section 3.2, the link capacities are set as follows: $c_{l_1} = c_{l_2} = c_{l_3} = c_{l_4} = \lambda = 20$ Mbps and $c_{l_5} = c_{l_6} = \lambda \times \tau = 20 \times \tau$ Mbps.

TABLE 1: Flow completion times (seconds) of the fat-tree experiments.

Flow	$\tau = 1$	$\tau = 4/3$	$\tau = 2$	Flow	$\tau = 1$	$\tau = 4/3$	$\tau = 2$
f_1	115	172	175	f_7	223	152	144
f_2	237	171	164	f_8	212	170	143
f_3	239	177	156	f_9	112	171	178
f_4	111	172	173	f_{10}	201	173	153
f_5	236	167	158	f_{11}	226	174	154
f_6	233	172	147	f_{12}	113	155	173
max()					239	177	178

As predicated by QTBS, the case $\tau = 1$ has flows operating at one of two bottleneck levels, close to the rates predicted by the bottleneck structure (2.5 Mbps for the upper-level flows and 5 Mbps for the lower-level flows, see Fig. 4b). This fat-tree design is inefficient for symmetric workloads since the flow completion time of the slowest flow is not minimal. Under this configuration, flow f_3 is the slowest flow and its completion time is 239 seconds. (See Table 1 for all flow completion time values.) If we want to maximize the rate of the slowest flow, QTBS tells us that the right tapering parameter value is $4/3$. This case is presented in Fig. 5b, which indeed shows how all flows perform at a very similar rate close to the theoretical value of 3.333 Mbps (see Fig. 4c). This configuration is optimal in that it minimizes the maximum completion time of any of the flows. In this experiment, the completion time of the slowest flow is 177 seconds, an improvement of 25.9% with respect to the case of $\tau = 1$. Fig. 5c shows the results for the case of a full fat-tree network, $\tau = 2$. Once again, as predicted by QTBS, this solution achieves about the same completion time as the case $\tau = 4/3$ (the slowest flow completes in 178 seconds), since in this configuration the leaf links become the bottlenecks and the extra bandwidth

added in the spine links does not produce any net benefit, as shown by the bottleneck structure in Fig. 4d. In summary, as predicted by QTBS, the case $\tau = 4/3$ constitutes an optimal design in that it is the least costly network that minimizes the maximum completion time of any of the flows.

Note that the existence of an optimal design with a tapering parameter $\tau = 4/3$ argues against some of the established conventional best practices in fat-tree networks. For instance, while a full fat-tree ($\tau = 2$) is considered to be universally efficient [6], the analysis of its bottleneck structure demonstrates that such design is in general inefficient when flows are regulated by a congestion-control protocol. This is because the fairness and throughput maximization objectives targeted by the congestion control algorithm effectively *bends* the solution space and, as a result, the optimal fat-tree design deviates from the general full fat-tree configuration. This result has implications in the design of data centers that use fat-tree topologies (also known as folded-Clos [5]). While in this section we have illustrated how QTBS can be used to optimize a simple fat-tree topology for the case of a symmetric workload pattern, the authors are currently working on deriving the general equations for the optimal design of fat-trees with arbitrary number of spine and leaf links and for generalized (non-symmetric) workload patterns. We will be presenting these results in a forthcoming paper.

3.3. Traffic Engineering: Accelerating Time-Bound Constrained Flows

Suppose now that our goal is to accelerate a certain flow $f_t \in \mathcal{F}$ in a network \mathcal{N} so it completes before a target time. A common application for the optimization of time-bound flows can be found in research and education networks, where users need to share data obtained from their experiments, often involving terabytes (or even petabytes) of information, with collaborators around the globe—e.g., when scientists at the European Organization for Nuclear Research (CERN) need to share data with other researchers using the LHCONE network [24] across the globe. Another common use case can be found in large scale data centers, where massive data backups need to be transferred between sites to ensure redundancy [20]. In this context, assume operators are only allowed to sacrifice the performance of a subset of flows $\mathcal{F}' \subset \mathcal{F} \setminus \{f_t\}$, considered to be of lower priority than f_t . What flows in \mathcal{F}' constitute an optimal choice to traffic-shape so as to accelerate f_t ? By what amount should the rate of such flows be reduced? And by what amount will flow f_t be accelerated?

To illustrate that we can use QTBS to resolve the above problem, we will use the topology of Google’s B4 network (Fig. 2a) introduced in Section 3.1. Assume the network is transporting eight flows, $F = \{f_1, f_2, \dots, f_8\}$, routed as shown in the Fig. 6. This is without loss of generality as we can apply the same procedure to optimize networks with arbitrary number of flows and topology. We will use the network’s bottleneck structure to identify an optimal strategy for accelerating an arbitrary flow in a network. Assume that

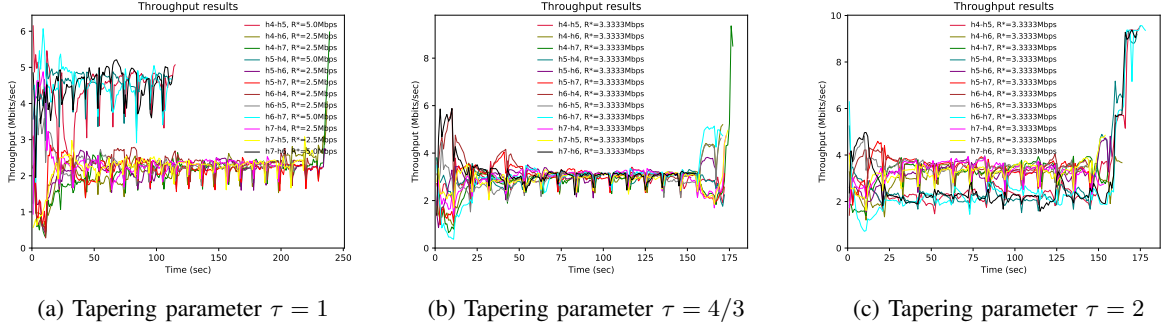


Figure 5: Optimizing bandwidth tapering on a 3-level binary fat-tree.

our objective is to accelerate flow f_7 (i.e., $f_t = f_7$) in Fig. 6—i.e., the transatlantic flow that connects data centers 8 and 12—to meet a certain flow completion time constraint. Assume also that in order to maximize the performance of f_7 we are allowed to traffic shape any of the flows in the set $\mathcal{F}' = \{f_1, f_3, f_4, f_8\}$. In other words, the set of flows in \mathcal{F}' are considered by the network operator to be of lower priority.

Fig. 7 displays the sequence of gradient graphs that lead to the acceleration of flow f_7 to meet its time constraint. The graphs include the values of the capacity c_l and fair share s_l next to each link vertex l and the rate r_f next to each flow vertex f . Fig. 7a corresponds to the gradient graph of the initial network configuration shown in Fig. 6 as computed by Algorithm 1. From Theorem 1, we know that only the flows that are ancestors to f_7 can have an effect on its performance. That means we can discard traffic shaping flow f_8 as that will have no impact. We can use the *ForwardGrad()* algorithm (Algorithm 2) to obtain the gradients of flow f_7 with respect to the flows in the low priority set \mathcal{F}' : $\nabla_{f_1}(f_7) = 2$, $\nabla_{f_3}(f_7) = -1$, $\nabla_{f_4}(f_7) = -2$, and $\nabla_{f_8}(f_7) = 0$. We are interested in finding the gradient of a flow in \mathcal{F}' that has the highest negative value, so that the traffic shaping of such a flow (i.e., the reduction of its rate) creates a maximal positive increase in the rate of f_7 . We have that flow f_4 has the highest negative gradient with a value of -2 , yielding an optimal traffic shaping decision. From Fig. 7a, it can be observed that the reduction of flow f_4 's rate creates a perturbation that propagates through the bottleneck structure via two different paths: $f_4 \rightarrow l_2 \rightarrow f_2 \rightarrow l_3 \rightarrow f_3 \rightarrow l_4 \rightarrow f_7$ and $f_4 \rightarrow l_4 \rightarrow f_7$. Each of these paths has an equal contribution to the gradient of value -1 , resulting in $\nabla_{f_4}(f_7) = -2$.

We can use the bottleneck structure again to calculate the exact value of the traffic shaper—i.e., the rate reduction applied to flow f_4 . The core idea is that traffic shaping flow f_4 constitutes an optimal decision as long as the bottleneck structure does not change, since a change in the structure would also imply a change in the gradients. As the rate of flow f_4 is reduced, some levels in the bottleneck structure will become further away from each other, while the others will become closer to each other. Thus, the latter set will fold if the rate reduction imposed by the traffic shaper is

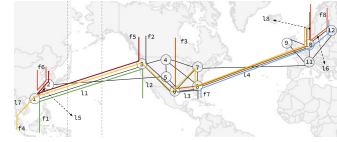


Figure 6: Network configuration used in Section 3.3.

large enough. The speed at which two links in the bottleneck structure get closer to (or further away from) each other is given by their gradients. In particular, if the traffic shaper reduces the rate of flow f_4 by an amount of ρ bps, then two links l and l' in the bottleneck structure will collide at a value of ρ that satisfies the equation $s_l - \rho \cdot \nabla_{f_4}(l) = s_{l'} - \rho \cdot \nabla_{f_4}(l')$. From the bottleneck structure (Fig. 7a) we can obtain the fair share values s_l and using the *ForwardGrad()* algorithm we can compute the link gradients $\nabla_{f_4}(l)$: $s_{l_2} = 5.125$; $s_{l_3} = 7.375$; $s_{l_4} = 10.25$; $s_{l_6} = 12.25$; $\nabla_{f_4}(l_2) = -1$; $\nabla_{f_4}(l_3) = 1$; $\nabla_{f_4}(l_4) = -2$; $\nabla_{f_4}(l_6) = 2$. Using these values, we have that the smallest value of ρ that satisfies the collision equation corresponds to the case $l = l_4$ and $l' = l_6$, yielding a ρ value of 0.5 (since $10.25 - \rho \cdot (-2) = 12.25 - \rho \cdot 2 \implies \rho = 0.5$). Thus, we conclude that to maximally increase the rate of flow f_7 , an optimal strategy is to decrease the rate of flow f_4 by an amount of 0.5 units of bandwidth. The resulting bottleneck structure is presented in Fig. 7b, where a new link l_7 has been added that corresponds to the new traffic shaper set to reduce the rate of flow f_4 by an amount of 0.5 (from 2.375 down to 1.875). Note that as expected, in this new bottleneck structure links l_4 and l_6 are folded into the same level and have the same fair share: $s_4 = s_6 = 11.25$.

Since f_7 has now two bottleneck links (l_4 and l_6), we cannot accelerate it further unless we increase the fair-shares of both. Using the new bottleneck structure (Fig. 7b), it is easy to see that this can be achieved by decreasing the rate of flows f_3 and f_8 , since the resulting link gradients are each negative $\nabla_{f_3}(l_4) = \nabla_{f_8}(l_6) = -1$. Thus, we add two new traffic shapers l_8 and l_9 to throttle the rate of flows f_3 and f_8 , respectively, down from their current rates of 6.875 and 11.25. That is: $c_{l_8} = 6.875 - \rho$ and $c_{l_9} = 11.25 - \rho$, for some traffic shaping amount ρ . In Fig. 7c, we show the resulting bottleneck structure when choosing a value of

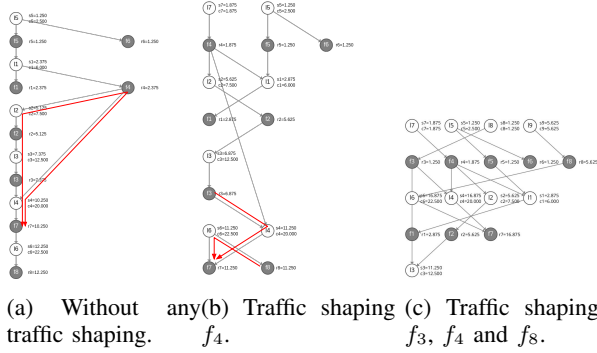


Figure 7: Bottleneck structures for each of the traffic shaping configurations used to accelerate flow f_7 .

$\rho = 5.625$ (so $c_{l_8} = 1.25$ and $c_{l_9} = 5.625$), which further accelerates the rate of flow f_7 to $r_7 = s_{l_4} - \rho \cdot \nabla_{f_3}(l_4) = s_{l_6} - \rho \cdot \nabla_{f_8}(l_6) = 11.25 - 5.625 \cdot (-1) = 16.875$. Note that there is some flexibility in choosing the value of this parameter, depending on the amount of acceleration required on flow f_7 . In this case, we chose a value that maximally accelerates flow f_7 while ensuring none of the flows that are traffic shaped receives a rate lower than any other flow. With this configuration, flow f_3 's rate is reduced to the lowest transmission rate among all flows in the network, but this value is no lower than the rate of flows f_5 and f_6 ($r_{f_3} = r_{f_5} = r_{f_6} = 1.25$). Thus, the flow completion time of the slowest flow is preserved throughout the transformations performed in this example.

In summary, a strategy to accelerate the performance of flow f_7 consists in traffic shaping the rates of flows f_3 , f_4 and f_8 down to 1.25, 1.875 and 5.625, respectively. Such a configuration results in a theoretical increase to the rate of flow f_7 from 10.25 to 16.875, while ensuring no flow performs at a rate lower than the slowest flow in the initial network configuration. Note that among all the low priority flows in \mathcal{F}' , in the above process we opted for not reducing the rate of flow f_1 . Indeed, the three bottleneck structures computed by this algorithm (Fig. 7) tell us that choosing to reduce the rate of flow f_1 would in fact have either a negative effect or no effect at all on the rate of flow f_7 , since the gradients $\nabla_{f_1}(f_7)$ for each structure are 2, 0 and 1, respectively—that is, a reduction on the rate of flow f_1 produces a non-positive impact on the rate of flow f_7 in all cases. Thus, the quantitative analysis resulting from the bottleneck structure of the network reveals not only the set of flows that should be traffic shaped, but also the flows that should *not* be traffic shaped, as doing so would actually hurt the performance of the flow we intend to accelerate. Note that this result challenges some of the established best practices for traffic engineering flows, which include many proposed algorithms that focus on reducing the rate of the heavy-hitter flows to improve high-priority flows. As shown in this example, without taking into account the bottleneck structure of a network, such algorithms may recommend a traffic shaping configuration that actually has the opposite

of the intended effect.

To empirically demonstrate the accuracy of QTBS in identifying the set of traffic shapers and their optimal rate, we reproduce the experiments described in this section using *Mininet-G2*. Fig. 8 illustrates the performance of the flows for each of the three traffic shaping configurations shown in Fig. 7 using the BBR congestion control algorithm. The legends in these figures describe the flows, where the notation $h_x - h_y$ means that the flow goes from host h_x to host h_y . To map the flows according to Fig. 6, we use the convention that host h_x is located in data center x . For instance, flow $h_8 - h_{12}$ in Fig. 8 corresponds with flow f_7 in Fig. 6, which starts at datacenter 8 and ends at datacenter 12. Table 2 shows the average transmission rate obtained for each of the flows and for each of the three experiments. Next to each experimental rate value, this table also includes the theoretical flow transmission rate according to the bottleneck structure. It is easy to see that these values match the transmission rate r_f shown next to each flow vertex (gray vertices) from the corresponding bottleneck structures in Fig. 7.

Fig. 8a shows the results of running the initial network without any traffic shapers, corresponding to the bottleneck structure in Fig. 7a. From Table 2, we see that all experimentally measured flow rates usually track their theoretical value from slightly below. Such an offset between experimental and theoretical rates is a characteristic that holds for all experiments, and is due to imperfections in the distributed nature of the congestion control algorithm (e.g., due to its inability to instantaneously converge to the optimal transmission rate or due to statistical packet drops produced by the asynchronous nature of the network). However, the table clearly demonstrates that the experimental rates behave according to the bottleneck structure of the network. This result is also reinforced by the fact that Jain's fairness index is above 0.99 for all experiments, as shown in Appendix G.

Fig. 8b shows the result of adding the first traffic shaper, configured to reduce the rate of flow f_4 by an amount of 0.5 Mbps. As predicted by QTBS, this increases the rate of flow f_7 (the purple flow $h_8 - h_{12}$ in Fig. 8), in this case from 9.51 to 9.81 Mbps (Table 2). Fig. 8c shows the result of adding two additional traffic shapers to reduce the rate of flows f_3 and f_4 by an amount of 5.625 Mbps, according to our quantitative analysis of the bottleneck structure. Recall that this configuration was designed to ensure a maximal increase in the rate of flow f_7 without decreasing any of the flows' rate below the rate of the slowest flow. We see this behavior in Fig. 8c, where flow f_7 (purple flow) has now the highest rate, while the flow completion time of the slowest flow remains at slightly above 400 seconds, throughout the three experiments (Fig. 8a, 8b and 8c). In summary, the combined effect of the three traffic shapers accelerates the observed rate of flow f_7 from 9.51 to 15.34 Mbps. As shown in Table 2, this result closely matches the behavior predicted by the bottleneck structure—that the rate would increase from 10.25 to 16.87 Mbps, while the observed maximum flow completion time of the network remains constant throughout the three experiments.

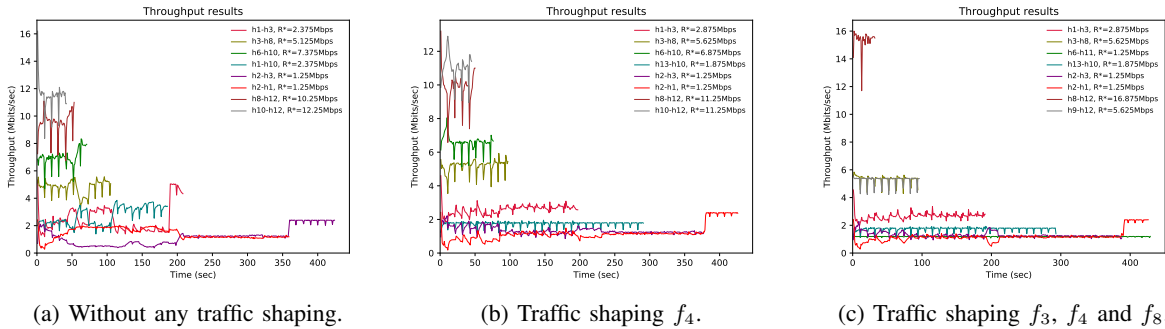


Figure 8: Flow performance obtained when deploying the traffic shapers to accelerate flow f_7 ($h_8 - h_{12}$).

TABLE 2: Experimental versus theoretical average flow transmission rate (units in Mbps).

Flow	Experiment 1	Experiment 2	Experiment 3
f_1	2.44 / 2.37	2.57 / 2.87	2.65 / 2.87
f_2	4.78 / 5.12	5.16 / 5.62	5.33 / 5.62
f_3	6.99 / 7.37	6.57 / 6.87	1.18 / 1.25
f_4	2.72 / 2.37	1.74 / 1.87	1.73 / 1.87
f_5	1.18 / 1.25	1.33 / 1.25	1.29 / 1.25
f_6	1.42 / 1.25	1.19 / 1.25	1.19 / 1.25
f_7	9.51 / 10.25	9.81 / 11.25	15.34 / 16.87
f_8	11.48 / 12.25	11.06 / 11.25	5.27 / 5.62

4. Related Work

The problem of congestion control is one of the most widely studied areas in data networks. The first congestion control algorithm for the Internet was introduced by Jacobson in [1] and implemented as part of the TCP protocol, initiating a more than three-decade long period of intense research. This has resulted in a long list of congestion control algorithms (e.g., [10], [7]), including the BBR algorithm recently proposed by Google [2]. All of these algorithms are based on the belief that the performance of a flow is solely characterized by the state of its bottleneck. In our work, we show that QTBS reveals a richer story of how such bottlenecks perform and interact with each other from a system-wide performance standpoint.

A well-known example of the traditional single-bottleneck view is the Mathis equation [25], which models the performance of a single TCP flow based on the equation $MSS/(RTT \cdot \sqrt{p})$, where MSS is the maximum segment size, RTT is the round trip time of the flow and p is the packet loss probability. This equation, however, does not take into account the system-wide properties of a network, including its topology, the routing and the interactions between flows. QTBS addresses this gap and provides a methodology to numerically estimate flow throughput. In future research we plan to incorporate the effects of latency and packet loss to QTBS.

The concept of bottleneck structure was recently introduced in [3]. That work focused on the qualitative properties of the bottleneck precedence graph (BPG), a structure that organizes the relationships among links. Our work focuses on the analysis of a bottleneck structure called the gradient

graph. The key difference between the gradient graph and the BPG is that the gradient graph describes the relationships among flows and links, not just links, providing a more comprehensive view of the network. As a result, the gradient graph provides a framework to quantify the interactions among flows and links, resulting in a new class of algorithms to optimize network performance. To the best of our knowledge, this paper presents the first quantitative theory of the analysis of bottleneck structures in data networks.

The problem of traffic engineering (TE) has also been widely studied and continues to be a very active area of research and development. Because QTBS provides a new approach to network optimization, it can be used co-located with existing TE frameworks, augmenting them with detailed information about the interactions among bottleneck links and flows. For instance, in [4], Google introduces Bandwidth Enforcer (BwE), a centralized bandwidth allocation infrastructure for wide area networking that targets high network utilization. QTBS complement tools like BwE by providing a view of the network’s bottleneck structure (for online or offline analysis) and providing traffic shaping and flow routing recommendations such as those presented in Sections 3.3 and 3.1.

5. Conclusions

The analytical strength of a bottleneck structure stems from its ability to capture the solution-space produced by a congestion-control algorithm taking into account the topological and routing constraints of the network. Based on this concept, we develop a quantitative theory of bottleneck structures (QTBS), a new mathematical framework that allows to optimize congestion-controlled networks by providing very efficient algorithms to compute derivatives on the performance parameters of links and flows. To explore the analytical power of QTBS, we use it to reveal insights in traffic engineering and network design problems that are themselves contributions to the literature. In one experiment, we use QTBS to develop a novel routing algorithm that identifies maximal throughput paths, enabling a scalable methodology to jointly solve the problems of routing and congestion control. In another experiment, we use QTBS to reveal the existence of optimal capacity allocations in

the spine links of a fat-tree network that outperform (in cost and/or performance) the traditional full fat-tree network designs found in some large-scale data centers and super-computers. In a third experiment, we demonstrate how to use bottleneck structures to compute the numerical values of optimal rate settings in traffic shapers to help improve the performance of high-priority flows. This paper positions the concept of bottleneck structures as a promising analytical framework to optimize network performance.

References

- [1] V. Jacobson, "Congestion Avoidance and Control," *SIGCOMM computer communication review*, vol. 18, no. 4, pp. 314–329, August 1988. [Online]. Available: <http://doi.acm.org/10.1145/52325.52356>
- [2] N. Cardwell, Y. Cheng, C. S. Gunn, S. H. Yeganeh, and V. Jacobson, "BBR: Congestion-Based Congestion Control," *ACM Queue*, vol. 14, no. 5, pp. 50:20–50:53, October 2016. [Online]. Available: <http://doi.acm.org/10.1145/3012426.3022184>
- [3] J. Ros-Giralt, A. Bohara, S. Yellamraju, M. H. Langston, R. Lethin, Y. Jiang, L. Tassiulas, J. Li, Y. Tan, and M. Veeraraghavan, "On the bottleneck structure of congestion-controlled networks," *Proc. ACM Meas. Anal. Comput. Syst.*, vol. 3, no. 3, Dec. 2019. [Online]. Available: <https://doi.org/10.1145/3366707>
- [4] A. Kumar, S. Jain, U. Naik, A. Raghuraman, N. Kasinadhuni, E. C. Zermano, C. S. Gunn, J. Ai, B. Carlin, M. Amaranidei-Stavila, M. Robin, A. Siganporia, S. Stuart, and A. Vahdat, "Bwe: Flexible, hierarchical bandwidth allocation for wan distributed computing," *SIGCOMM Comput. Commun. Rev.*, vol. 45, no. 4, p. 1–14, Aug. 2015. [Online]. Available: <https://doi.org/10.1145/2829988.2787478>
- [5] M. Al-Fares, A. Loukissas, and A. Vahdat, "A scalable, commodity data center network architecture," in *Proceedings of the ACM SIGCOMM 2008 Conference on Data Communication*, ser. SIGCOMM '08. New York, NY, USA: Association for Computing Machinery, 2008, p. 63–74. [Online]. Available: <https://doi.org/10.1145/1402958.1402967>
- [6] C. E. Leiserson, "Fat-trees: universal networks for hardware-efficient supercomputing," *IEEE transactions on Computers*, vol. 100, no. 10, pp. 892–901, 1985.
- [7] S. Ha, I. Rhee, and L. Xu, "CUBIC: A New TCP-friendly High-speed TCP Variant," *SIGOPS operating systems review*, vol. 42, no. 5, pp. 64–74, July 2008. [Online]. Available: <http://doi.acm.org/10.1145/1400097.1400105>
- [8] D. P. Bertsekas and R. G. Gallager, *Data Networks*. Englewood Cliffs, New Jersey 07632: Prentice-Hall Inc., 1992, vol. 2.
- [9] F. P. Kelly, A. K. Maulloo, and D. K. H. Tan, "Rate Control for Communication Networks: Shadow Prices, Proportional Fairness and Stability," *Journal of the Operational Research society*, vol. 49, no. 3, pp. 237–252, March 1998. [Online]. Available: <https://doi.org/10.1057/palgrave.jors.2600523>
- [10] K. Fall and S. Floyd, "Simulation-based Comparisons of Tahoe, Reno and SACK TCP," *SIGCOMM Computer Communication Review*, vol. 26, no. 3, pp. 5–21, July 1996. [Online]. Available: <http://doi.acm.org/10.1145/235160.235162>
- [11] D. Kreutz, F. M. V. Ramos, P. E. Verissimo, C. E. Rothenberg, S. Azodolmolky, and S. Uhlig, "Software-defined networking: A comprehensive survey," *Proceedings of the IEEE*, vol. 103, no. 1, pp. 14–76, 2015.
- [12] R. D. Neidinger, "Introduction to automatic differentiation and matlab object-oriented programming," *SIAM Rev.*, vol. 52, no. 3, p. 545–563, Aug. 2010. [Online]. Available: <https://doi.org/10.1137/080743627>
- [13] (2019) Mininet-g2: Mininet extensions to support the analysis of the bottleneck structure of networks. [url]. [Online]. Available: <https://github.com/reservoirirlabs/g2-mininet>
- [14] Mininet. (2019) Mininet: An instant virtual network on your laptop (or other pc). [Online]. Available: <http://mininet.org/>
- [15] R. Jain, D.-M. W. Chiu, and W. R. Hawe, "A quantitative measure of fairness and discrimination for resource allocation in shared computer systems," *CoRR*, vol. cs.NI/9809099, 1998. [Online]. Available: <http://arxiv.org/abs/cs.NI/9809099>
- [16] S. H. Y. Rekhter, T. Li, "A border gateway protocol 4 (bgp-4)," *Internet Engineering Task Force (IETF), Request for Comments*, 2006.
- [17] A. Eryilmaz and R. Srikant, "Joint congestion control, routing, and mac for stability and fairness in wireless networks," *IEEE Journal on Selected Areas in Communications*, vol. 24, no. 8, pp. 1514–1524, 2006.
- [18] J. Liu and H. D. Sherali, "A distributed newton's method for joint multi-hop routing and flow control: Theory and algorithm," in *2012 Proceedings IEEE INFOCOM*, 2012, pp. 2489–2497.
- [19] L. Tassiulas and A. Ephremides, "Stability properties of constrained queueing systems and scheduling policies for maximum throughput in multihop radio networks," *IEEE Transactions on Automatic Control*, vol. 37, no. 12, pp. 1936–1948, 1992.
- [20] S. Jain, A. Kumar, S. Mandal, J. Ong, L. Poutievski, A. Singh, S. Venkata, J. Wanderer, J. Zhou, M. Zhu, J. Zolla, U. Hölzle, S. Stuart, and A. Vahdat, "B4: Experience with a Globally-Deployed Software Defined WAN," *SIGCOMM Computer Communication Review*, vol. 43, no. 4, pp. 3–14, August 2013. [Online]. Available: <http://doi.acm.org/10.1145/2534169.2486019>
- [21] G. Michelogiannakis, Y. Shen, M. Y. Teh, X. Meng, B. Aivazi, T. Groves, J. Shalf, M. Glick, M. Ghobadi, L. Dennison, and K. Bergman, "Bandwidth steering in hpc using silicon nanophotonics," in *Proceedings of the International Conference for High Performance Computing, Networking, Storage and Analysis*, ser. SC '19. New York, NY, USA: Association for Computing Machinery, 2019. [Online]. Available: <https://doi.org/10.1145/3295500.3356145>
- [22] W. E. Denzel, J. Li, P. Walker, and Y. Jin, "A framework for end-to-end simulation of high-performance computing systems," *Simulation*, vol. 86, no. 5-6, pp. 331–350, 2010.
- [23] E. A. León, I. Karlin, A. Bhatele, S. H. Langer, C. Chambreaux, L. H. Howell, T. D'Hoooge, and M. L. Leininger, "Characterizing parallel scientific applications on commodity clusters: An empirical study of a tapered fat-tree," in *SC'16: Proceedings of the International Conference for High Performance Computing, Networking, Storage and Analysis*. IEEE, 2016, pp. 909–920.
- [24] E. Martelli and S. Stancu, "Lhcopn and lhcone: status and future evolution," in *Journal of Physics: Conference Series*, vol. 664, no. 5. IOP Publishing, 2015, p. 052025.
- [25] M. Mathis, J. Semke, J. Mahdavi, and T. Ott, "The macroscopic behavior of the tcp congestion avoidance algorithm," *SIGCOMM Comput. Commun. Rev.*, vol. 27, no. 3, pp. 67–82, Jul. 1997. [Online]. Available: <http://doi.acm.org/10.1145/263932.264023>
- [26] T. H. Cormen, C. E. Leiserson, R. L. Rivest, and C. Stein, *Introduction to Algorithms, Third Edition*, 3rd ed. The MIT Press, 2009.
- [27] N. R. POX, "The pox network software platform," 2019, =<https://noxrepo.github.io/pox-doc/html/>, Last accessed 09/24/2019.
- [28] Iperf.fr. (2019) iperf - the ultimate speed test tool for tcp, udp and sctp. [Online]. Available: <https://iperf.fr/>
- [29] P. Phaal, S. Panchen, and N. McKee, "sFlow Specifications, InMon Corporation," *IETF RFC 3176*, 2001.
- [30] B. Claise, G. Sadasivan, V. Valluri, and M. Djernaes. (2004) Netflow specifications, cisco systems. [Online]. Available: <https://www.ietf.org/rfc/rfc3954.txt>
- [31] J. Case, M. Fedor, M. Schoffstall, and J. Davin. (1990) A simple network management protocol (snmp). [Online]. Available: <https://tools.ietf.org/html/rfc1157>

6. Appendices

Appendix

1. Generalization to Max-min Fairness

Lemma 3. *If a link is a bottleneck in the max-min sense [8], then it is also a bottleneck according to Definition 2, but not vice-versa.*

Proof. Bertsekas and Gallager [8] proved that if a flow f is bottlenecked at link l in the max-min sense, then such a flow must traverse link l and its rate is equal to the link's fair share, $r_f = s_l$. Since a change in the capacity of a link always leads to a change in its fair share, i.e. $\partial s_l / \partial c_l \neq 0$, this necessarily implies $\partial r_f / \partial c_l \neq 0$. Thus, f is also bottlenecked at link l in the sense of Definition 2. The reverse, however, does not hold because Definition 2 does not require that $r_f = s_l$ for a flow f bottlenecked at link l . (It can be seen that this is also true for other definitions of bottleneck. For instance, a flow that is bottlenecked at a link according to proportional fairness [9], is also bottlenecked according to Definition 2, but the reserve is also not true.) \square

2. Proof of Theorem 1: Propagation of Network Perturbations

Let $x, y \in \mathcal{L} \cup \mathcal{F}$ be a pair of links or flows in the network. Then a perturbation in the capacity c_x (for $x \in \mathcal{L}$) or transmission rate r_x (for $x \in \mathcal{F}$) of x will affect the fair share s_y (for $y \in \mathcal{L}$) or transmission rate r_y (for $y \in \mathcal{F}$) of y if only if there exists a directed path from x to y in the gradient graph.

Proof. Consider the case $x = l \in \mathcal{L}$ and assume link l is affected by a perturbation in its capacity. From Definition 2, we have that $\partial r_{f^*} / \partial c_l \neq 0$, for any flow f^* bottleneck at link l . From Definition 4, these correspond to all flows f^* for which there exists an edge (l, f^*) in \mathcal{G} . Let f_1 be any of these flows and assume Δ_{f_1} is its drift. Such drift will induce a perturbation in all the links traversed by f_1 . From Definition 4, this corresponds to all the links l^* for which there exists an edge (f_1, l^*) in \mathcal{G} . This process of perturbation followed by a propagation repeats itself, affecting all the link and flow vertices that can be reached from link l through a directed path in the gradient graph, and ending at leaf vertices. This demonstrates the sufficient condition of the theorem. The necessary condition is also true because, from the definition of region of influence (Definition 5), none of the links and flows outside $\mathcal{R}(l)$ will be affected by the perturbation. The proof for the case $x = f \in \mathcal{F}$ follows the same argument except that the initial perturbation is applied on the rate of flow f . \square

3. Proof of Theorem 2: Correctness of *GradientGraph()*

Let $\mathcal{N} = \langle \mathcal{L}, \mathcal{F}, \{c_l, \forall l \in \mathcal{L}\} \rangle$ be a network and let \mathcal{G} be the corresponding gradient graph. Let $x \in \mathcal{L} \cup \mathcal{F}$.

After running Algorithm 2, $\Delta s_l = \nabla_x(l)$ for all $l \in \mathcal{L}$, and $\Delta r_f = \nabla_x(f)$ for all $f \in \mathcal{F}$.

Proof. Assume without loss of generality that $x \in \mathcal{L}$. Our goal is to prove:

$$\begin{aligned} \frac{\partial r_f}{\partial c_x} &= \Delta r_f & \forall f \in \mathcal{F} \\ \frac{\partial s_l}{\partial c_x} &= \Delta s_l & \forall l \in \mathcal{L} \end{aligned}$$

This is equivalent to showing that, for sufficiently small δ , if we perturbed the capacity of link x , $c'_x = c_x + \delta$, and recomputed all the flows' rates and links' fair shares using *GradientGraph()*, we would get:

$$\begin{aligned} r'_f &= r_f + \Delta r_f \cdot \delta & \forall f \in \mathcal{F} \\ s'_l &= s_l + \Delta s_l \cdot \delta & \forall l \in \mathcal{L} \end{aligned}$$

Let $y \in \mathcal{L} \cup \mathcal{F}$. There are two cases. First, assume $y \notin \mathcal{R}(x)$, where $\mathcal{R}(x)$ is the region of influence of x , then by definition there is no directed path from x to y . The algorithm only processes vertices that lie on a directed path from vertex x . Thus, if $y \in \mathcal{L}$, $\Delta s_y = 0$ (line 3) and if $y \in \mathcal{F}$, $\Delta r_y = 0$ (line 2). Moreover, by Theorem 1, y is not affected by the perturbation of c_x . That is, $s'_l = s_l$ or $r'_f = r_f$. Thus the equations hold.

Now let $y \in \mathcal{R}(x)$. We proceed by induction. As a base case, let $y = x$. The amount of leftover bandwidth at node x , which is called a_x in the *GradientGraph()* Algorithm, is the capacity c_x minus the rates of vertices that lie outside the region of influence of x , since they are not bottlenecked at x (see *GradientGraph()* lines 3 and 16). Thus $a'_x = a_x + (c'_x - c_x) = a_x + \delta$. The fair share rate of x is $s_x = a_x / |\mathcal{F}_x \setminus \mathcal{V}|$ (line 17 of *GradientGraph()*), where \mathcal{V} is the set of vertices that were added to the gradient graph before x . These necessarily lie outside the region of influence of x , so this set is the same after the perturbation. Indeed, $\mathcal{F}_x \setminus \mathcal{V}$ is the set of flows which are bottlenecked at x , which is also the set of successors of x . Thus,

$$s'_x = \frac{a_x + \delta}{|\mathcal{F}_x \setminus \mathcal{V}|} = s_x + \frac{\delta}{\sigma(x, \mathcal{G})} = s_x + \Delta s_x \cdot \delta$$

where $\sigma(x, \mathcal{G})$ corresponds to the set of successors of node x as indicated by the gradient graph \mathcal{G} . Thus, the equations hold for x .

Now assume the equations hold for all vertices which are added to the new gradient graph prior to vertex y . First, assume $y \in \mathcal{F}$. Then r'_y will be the minimum fair share rate of the links it traverses, that is, $\min s'_l$ for all $l \in \mathcal{L}_y$. However, it suffices to take the minimum over links which were predecessors (bottlenecks) of y in the original gradient graph (these links' fair shares were strictly smaller than those of the other vertices that y traverses, so after an infinitesimally small perturbation they will remain strictly smaller). Thus,

$$r'_y = \min_{l \in \pi(y, \mathcal{G})} s'_l = \min_{l \in \pi(y, \mathcal{G})} (s_l + \Delta s_l \cdot \delta)$$

where $\pi(y, \mathcal{G})$ corresponds to the set of predecessors of node y as indicated by the gradient graph \mathcal{G} . Now we can substitute $s'_l = s_l + \Delta s_l \cdot \delta$ because of the induction hypothesis. If y had multiple bottleneck links in the original graph, then they all had the same fairshare. That is, $s_l = r_y$ for all $l \in \pi(y, \mathcal{G})$. So

$$r'_y = r_y + \left[\min_{l \in \pi(y, \mathcal{G})} \Delta s_l \right] \cdot \delta$$

Combining this with line 23 of *ForwardGraph()*,

$$\begin{aligned} \Delta r_y &= \min_{l \in \pi(y, \mathcal{G})} \Delta s_l \\ \implies r'_y &= r_y + \Delta r_y \cdot \delta \end{aligned}$$

which is what we wanted to prove under the assumption that $y \in \mathcal{F}$. Now, assume $y \in \mathcal{L}$. The old fair share of y was its available capacity (called a_y in *GradientGraph()*) divided by the number of flows that it bottlenecked, $|\sigma(y, \mathcal{G})|$. That is,

$$s_y = \frac{a_y}{|\sigma(y, \mathcal{G})|} = \frac{c_y - \sum_{f \in \mathcal{F}_y \setminus \sigma(y, \mathcal{G})} r_f}{|\sigma(y, \mathcal{G})|}$$

(See *GradientGraph()* lines 3, 16, and 17). The new fair share is

$$s'_y = \frac{a'_y}{|\sigma(y, \mathcal{G}')|} = \frac{c'_y - \sum_{f \in \mathcal{F}_y \setminus \sigma(y, \mathcal{G}')} r'_f}{|\sigma(y, \mathcal{G}')|}$$

The capacity of y has not changed (unless $y = x$, which we already considered) so $c'_y = c_y$. As a result of the perturbation, some flows which used to be bottlenecked at y may no longer be (if they were perturbed directly, or if they had a second bottleneck that was affected). But no new bottlenecked flows were created, since flows that were not bottlenecked at y before had rates strictly smaller than s_y , and the perturbation is infinitesimally small. Let

$$T_y = \sigma(y, \mathcal{G}) \setminus \sigma(y, \mathcal{G}')$$

be the flows that were bottlenecked at y , but whose rate was reduced an infinitesimal amount by the perturbation, so that they no longer are. Then with some algebraic manipulation,

$$\begin{aligned} s'_y &= \frac{c_y - \sum_{f \in \mathcal{F}_y \setminus \sigma(y, \mathcal{G}')} r'_f}{|\sigma(y, \mathcal{G}')|} \\ &= \frac{c_y - \left(\sum_{f \in \mathcal{F}_y \setminus \sigma(y, \mathcal{G}')} r_f \right) - \left(\sum_{f \in \mathcal{F}_y \setminus \sigma(y, \mathcal{G}')} r'_f - r_f \right)}{|\sigma(y, \mathcal{G}')|} \\ &= \frac{c_y - \left(\sum_{f \in \mathcal{F}_y \setminus \sigma(y, \mathcal{G}')} r_f \right) - \left(\sum_{f \in T_y} r_f \right)}{|\sigma(y, \mathcal{G}')|} \\ &\quad - \frac{\left(\sum_{f \in \mathcal{F}_y \setminus \sigma(y, \mathcal{G}')} r'_f - r_f \right)}{|\sigma(y, \mathcal{G}')|} \\ &= \frac{a_y - |T_y| s_y}{|\sigma(y, \mathcal{G})| - |T_y|} - \frac{\left(\sum_{f \in \mathcal{F}_y \setminus \sigma(y, \mathcal{G}')} r'_f - r_f \right)}{|\sigma(y, \mathcal{G}')|} \end{aligned}$$

where in the last line, we have used the fact that $r_f = s_y$ for all $f \in T_y$, since each of these flows used to be bottlenecked at y before the perturbation. Furthermore, since

$$s_y = \frac{a_y}{|\sigma(y, \mathcal{G})|}$$

the first term in the last line above simplifies as follows:

$$\frac{a_y - |T_y| s_y}{|\sigma(y, \mathcal{G})| - |T_y|} = \frac{|\sigma(y, \mathcal{G})| s_y - |T_y| s_y}{|\sigma(y, \mathcal{G})| - |T_y|} = s_y$$

Thus

$$s'_y = s_y - \frac{\left(\sum_{f \in \mathcal{F}_y \setminus \sigma(y, \mathcal{G}')} r'_f - r_f \right)}{|\sigma(y, \mathcal{G}')|}$$

In *ForwardGrad()*, each of the flow vertices in $\mathcal{F}_y \setminus \sigma(y, \mathcal{G}')$ has a smaller key in the heap than y does, since they either had a smaller rate than s_y before, or they have a more negative drift than y does (so their $\Delta r_f < \Delta s_y$). This means that they will be processed before y , and that $\Delta r_f = r'_f - r_f$. Thus, by the time y is processed,

$$\Delta c_y = - \sum_{f \in \mathcal{F}_y \setminus \sigma(y, \mathcal{G}')} \Delta r_f = - \sum_{f \in \mathcal{F}_y \setminus \sigma(y, \mathcal{G}')} (r'_f - r_f) / \delta$$

(see line 26) where we have $r'_f = r_f + \Delta r_f \cdot \delta$ by the induction hypothesis. As we just reasoned, by the time y is processed, all the nodes in T_y have been visited already for the same reason. Thus,

$$|\sigma(y, \mathcal{G}) \setminus V| = |\sigma(y, \mathcal{G}) \setminus T_y| = |\sigma(y, \mathcal{G}')|$$

Combining with line 27,

$$\begin{aligned} \Delta s_y &= \frac{\Delta c_y}{|\sigma(y, \mathcal{G}) \setminus V|} \\ \implies s_y &= s_y + \frac{\Delta c_y \cdot \delta}{|\sigma(y, \mathcal{G}) \setminus V|} = s_y + \Delta s_y \cdot \delta \end{aligned}$$

which is what we wanted to prove. By induction, $\Delta s_l = \partial s_l / \partial c_x$ and $\Delta r_f = \partial r_f / \partial c_x$ for all links l and all flows f in the region of influence of x . \square

4. Proof of Theorem 3: Time Complexity of *ForwardGrad()*

Let $x \in \mathcal{L} \cup \mathcal{F}$. Then Algorithm 2 finds the gradients of all links and flows in the network with respect to x in time $O(|\mathcal{R}(x)| \cdot \log |\mathcal{R}(x)|)$.

Proof. Algorithm 2 only adds vertices to the heap (line 24 and 28) if they are neighbors of a previously visited vertex, so it only visits vertices in the region of influence $\mathcal{R}(x)$. Moreover, the algorithm only visits each node once (lines 15 - 16). The only operation that is not constant-time is updating the heap (lines 24 and 28). Since the heap has at most $|\mathcal{R}(x)|$ elements, each of these operations takes $\log |\mathcal{R}(x)|$, so the total runtime of the algorithm is $O(|\mathcal{R}(x)| \cdot \log |\mathcal{R}(x)|)$. \square

5. Proof of Lemma 1: Time Complexity of GradientGraph()

The time complexity of running GradientGraph() is $O(|\mathcal{L}| \log |\mathcal{L}| \cdot H)$, where H is the maximum number of flows that traverse a single link.

Proof. Note that each statement in the algorithm runs in constant time except for lines 5, 8, and 18. Each is an operation on a heap of size at most $|\mathcal{L}|$, so each will run in $\log |\mathcal{L}|$ time. Lines 5 and 8 will each run $|\mathcal{L}|$ times, since the two outer loops run at most once for each link. Line 18 will run at most once for every pair of a link with a flow that traverses it. Note that this value is less than the number of edges that are added to the gradient graph in lines 10 and 15. Thus, the number of times line 18 is run is bounded by $|\mathcal{L}| \cdot H$, where H is the maximum number of flows that traverse a single link. Thus, in total, the algorithm runs in time $O(H|\mathcal{L}| \log(|\mathcal{L}|))$. \square

6. Proof of Property 1: Gradient Bound

Let $\mathcal{N} = \langle \mathcal{L}, \mathcal{F}, \{c_l, \forall l \in \mathcal{L}\} \rangle$ be a network and let \mathcal{G} be its gradient graph. Let δ be an infinitesimally small perturbation performed on a flow or link $x \in \mathcal{L} \cup \mathcal{F}$, producing a drift Δ_y , for all $y \in \mathcal{L} \cup \mathcal{F}$. Then, $\nabla_x(y) = \Delta_y / \delta \leq d^{D(\mathcal{G})/4}$, where $D(\mathcal{G})$ is the diameter of a graph \mathcal{X} and d is the maximum indegree and outdegree of any vertex in the graph.

Proof. From the invariants of the flow and link equations, we observe that the absolute value of a perturbation can only increase when traversing a link vertex. This is because the flow equation $\Delta_f = \min_{l \in P_f} \Delta_l$ necessarily implies that the size of the perturbation will either stay the same or decrease. The link equation $\Delta_l = -\sum_{f \in P_l} \Delta_f / |S_l|$, however, allows perturbations to grow in absolute value. This will happen whenever the sum of the flow drifts arriving at a link vertex is larger than the outdegree of such vertex: $\sum_{f \in P_l} \Delta_f > |S_l|$. The size of the perturbation will in fact maximally increase when the link outdegree is 1 and the sum of the flow drifts arriving at it is maximal. This is achieved when the bottleneck structure is configured with flows having an outdegree of d and links having an indegree of d , connected by a stage of inter-medium links and flows of indegree and outdegree equal to 1, as shown in Fig. A1. Concatenating this bottleneck structure block, we have that at each block the perturbation increases d times. Because the length of this block is 4, there are a maximum of $D(\mathcal{G})/4$ blocks, where $D(\mathcal{G})$ is the diameter of the gradient graph. This leads to the upper bound $\nabla_x(y) = \Delta_y / \delta \leq d^{D(\mathcal{G})/4}$. \square

7. Lemmas to Demonstrate the Correctness of the MaxRatePath Algorithm

Lemma 4. Flow rate decay with incremental hop count. Let $\mathcal{N} = \langle \mathcal{L}, \mathcal{F}, \{c_l, \forall l \in \mathcal{L}\} \rangle$ be a network and let r_f be

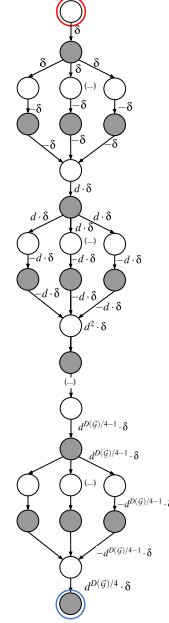


Figure A1: Bottleneck structure with maximal drift used to prove the gradient bound lemma.

the transmission rate of a flow $f \in \mathcal{F}$. Let r'_f be the new transmission rate of flow f after we extend it to traverse an additional link $l^* \in \mathcal{L} \setminus f$. Then, $r'_f \leq r_f$.

Proof. Fig. A2-a shows the initial situation of the lemma, with flow f bottlenecked at a link l . Since the transmission rate of flow f is r_f , we have that $s_l = r_f$. Suppose that we extend flow f to traverse an extra link $l^* \in \mathcal{L} \setminus f$. Now consider the next set of transformations applied on the network:

- 1) Create a new flow f^* configured to only traverse link l^* .
- 2) Add a traffic shaper l_s to flow f^* and set its rate to zero, i.e. $s_{l_s} = c_{l_s} = 0$.
- 3) Increase the rate of the traffic shaper until either (a) l^* becomes a bottleneck of f^* or (b) $s_{l_s} = s_l$.
- 4) Connect flows f and f^* together.
- 5) Remove the traffic shaper l_s .

It is easy to see that the above process yields a bottleneck structure that is the same as if flow f had been extended to traverse the extra link l^* , since at the end of these steps the two flows f and f^* are merged into a single flow (effectively extending flow f to traverse the additional link l^*) and the traffic shaper is removed.

Let us now derive the bottleneck structure of the network after applying the above transformations. Steps (1) and (2) are shown in Fig. A2-b. In step (3), as we increase the capacity of the traffic shaper s_{l_s} , the rate of flow f^* increases at the same pace. Suppose that condition (3-a) holds so that l^* becomes a bottleneck of f^* . This situation is shown in Fig. A2-c.1. Since flow f^* is bottlenecked at both links l^* and l_s , we have that $s_{l^*} = s_{l_s}$. Because

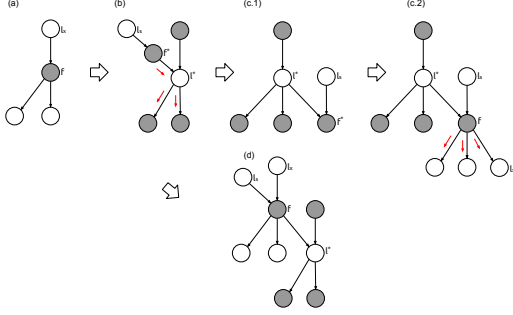


Figure A2: Bottleneck structures transformations used to demonstrate that adding a new link to a flow cannot increment its transmission rate.

condition (3-b) does not hold, it must also be that $s_{l_s} < s_l$, which then implies $s_{l^*} < s_l$. This necessarily means that, in step (4), the merging of the two flows f and f^* leads to the bottleneck structure shown in Fig. A2-c.2, whereby the new flow f is no longer bottlenecked at link l and, instead, it becomes bottlenecked at link l^* . Thus, we have that $r'_f = s_{l^*} < s_l = r_f$. Note that in this case, the ripple effects of extending flow f to traverse the extra link l^* affected the performance of link l , resulting in an increase of its fair share s_l value.

Assume instead that condition (3-b) holds so that $s_{l_s} = s_l$. In this case, the merging of flows f and f^* in step (4) leads to the bottleneck structure in Fig. A2-d, whereby flow f continues to be bottlenecked at link l and, thus, $r'_f = s_l = r_f$. Note that in this case, link l was unaffected by the ripple effects of extending flow f to traverse the extra link l^* .

Finally, in step 5 we can freely remove the traffic shaper l_s from the network without producing any ripple effect, since flow f is also bottlenecked at either link l^* (case 3-a) or link l (case 3-b).

In conclusion, we have that at the end of this process, $r'_f \leq r_f$. \square

Corollary 1. *New bottleneck with incremental hop count.* Let $\mathcal{N} = \langle \mathcal{L}, \mathcal{F}, \{c_l, \forall l \in \mathcal{L}\} \rangle$ be a network and let r_f be the transmission rate of a flow $f \in \mathcal{F}$. Let r'_f be the new transmission rate of flow f after we extend it to traverse an additional link $l^* \in \mathcal{L} \setminus f$. If, $r'_f < r_f$, then the newly extended flow is bottlenecked at link l^* .

Proof. This result is a direct consequence of Lemma 4, since the condition $r'_f < r_f$ corresponds to case (3-a), which leads to the bottleneck structure in Fig. A2-c.2. \square

LEMMA 2. *Let $\mathcal{N} = \langle \mathcal{L}, \mathcal{F}, \{c_l, \forall l \in \mathcal{L}\} \rangle$ be a network and \mathcal{U} the set of its routers. Suppose that f and f' are two flows not in \mathcal{F} that originate at router u_s and end at router u_d . Then $f = \text{MaxRatePath}(\mathcal{N}, \mathcal{U}, u_s, u_d)$ implies $r_f \geq r_{f'}$.*

Proof. Consider the network configuration in Fig. A3 and assume that routing data from router u_s to u_x using flow f_1

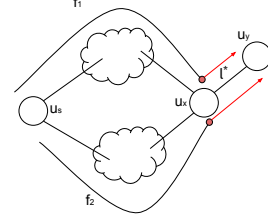


Figure A3: In the MaxRatePath algorithm, adding a new link to a flow preserves the correctness of the previous high-throughput path decisions.

leads to a higher transmission rate than using flow f_2 , $r_{f_1} > r_{f_2}$. Since the MaxRatePath algorithm uses the inverse of the rate as the path cost metric, this implies that $d_{f_1} < d_{f_2}$, where we use the notation d_f to denote the cost of using flow f to route traffic through the network. To demonstrate the correctness of the algorithm, we need to show that $d_{f_1} < d_{f_2}$ implies $d_{f_1 \cup \{l^*\}} \leq d_{f_2 \cup \{l^*\}}$, since this condition is enough to demonstrate convergence in the Dijkstra algorithm [26].

We will assume that $d_{f_1} < d_{f_2}$ and $d_{f_1 \cup \{l^*\}} > d_{f_2 \cup \{l^*\}}$ are both true and arrive at a contradiction. From Lemma 4 we have that $d_{f_2} \leq d_{f_2 \cup \{l^*\}}$. This implies that $d_{f_1 \cup \{l^*\}} > d_{f_2 \cup \{l^*\}} \geq d_{f_2} > d_{f_1}$. Using Corollary 1, it must be that l^* is the bottleneck of the flow $f_1 \cup \{l^*\}$. Now since flow $f_2 \cup \{l^*\}$ also traverses link l^* , it must be that its rate cannot be higher than that of flow $f_1 \cup \{l^*\}$. But this implies $d_{f_1 \cup \{l^*\}} \leq d_{f_2 \cup \{l^*\}}$, arriving at a contradiction. \square

The Mininet-G2 tool [13] provides a powerful, flexible interface to emulate networks of choice with customizable topology, routing and traffic flow configurations. It uses Mininet [14] and the POX SDN controller [27] to create such highly customizable networks. It also uses iPerf [28] internally to generate network traffic and offers an interface to configure various flow parameters such as the source and destination hosts, start time, and data size, among others. Mininet-G2 also offers an integration with sFlow-RT [29] agent that enables real-time access to traffic flows from Mininet emulated network. Since Mininet uses real, production grade TCP/IP stack from the Linux kernel, it proves to be an ideal testbed to run experiments using congestion control protocols such as BBR and Cubic to study bottleneck structures and flow performance in a realistic way. Apart from its flexible configuration interface, Mininet-G2 also offers a set of useful utilities to compute and plot various performance metrics such as instantaneous network throughput, flow convergence time, flow completion time, Jain's fairness index among others for a given experiment.

Tables 3, 4 and 5 and Fig. A4 and A5 present the results for the experiments described in Sections 3.3, 3.1 and 3.2 when using Cubic as the congestion control protocol.

Jain's index [15] is a metric that rates the fairness of a set of values x_1, x_2, \dots, x_n according to the following equation:

$$\mathcal{J}(x_1, x_2, \dots, x_n) = \frac{(\sum_{i=1}^n x_i)^2}{n \cdot \sum_{i=1}^n x_i^2} = \frac{\bar{x}^2}{\overline{x^2}}$$

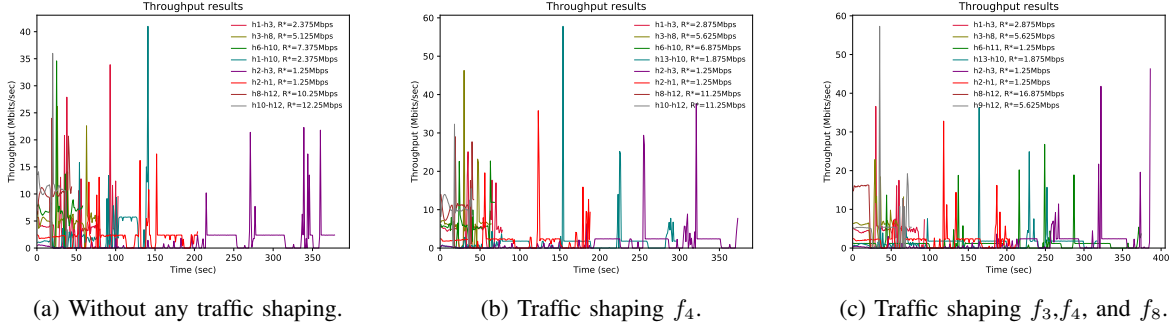


Figure A4: Traffic shaping schedule to accelerate flow f_7 ($h_8 - h_{12}$) (TCP Cubic).

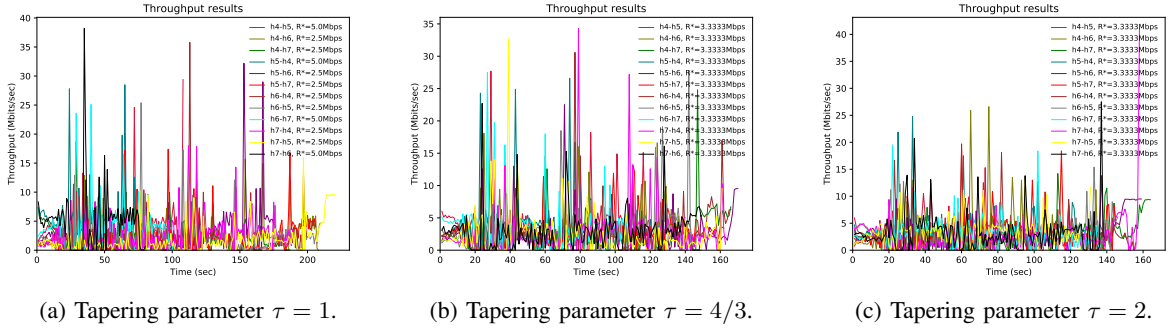


Figure A5: Optimizing bandwidth tapering on a 3-level binary fat-tree (TCP Cubic).

TABLE 3: Experimental versus theoretical average flow transmission rate (units in Mbps) for Section. 3.3 when using TCP Cubic.

Flow	Experiment 1	Experiment 2	Experiment 3
f_1	3.91 / 2.37	5.10 / 2.87	4.43 / 2.87
f_2	5.26 / 5.12	6.39 / 5.62	5.94 / 5.62
f_3	6.83 / 7.37	6.17 / 6.87	1.04 / 1.25
f_4	2.74 / 2.37	1.40 / 1.87	1.38 / 1.87
f_5	1.09 / 1.25	1.15 / 1.25	1.14 / 1.25
f_6	2.04 / 1.25	2.10 / 1.25	2.01 / 1.25
f_7	10.22 / 10.25	10.49 / 11.25	14.4 / 16.87
f_8	10.62 / 12.25	10.58 / 11.25	5.37 / 5.62

TABLE 4: Experimental versus theoretical average flow transmission rate (units in Mbps) for Section. 3.1 when using TCP Cubic.

Flow	Shortest path	Longer path	Flow	Shortest path	Longer path
f_1	0.917 / 1.428	0.962 / 1.666	f_{14}	1.841 / 1.666	1.864 / 1.666
f_2	1.296 / 1.666	1.278 / 1.666	f_{15}	1.284 / 1.666	1.230 / 1.666
f_3	1.202 / 1.428	1.315 / 1.666	f_{16}	1.294 / 1.666	1.292 / 1.666
f_4	0.897 / 1.428	0.9685 / 1.666	f_{17}	2.035 / 2.142	2.132 / 2.142
f_5	1.186 / 1.428	1.336 / 1.666	f_{18}	2.097 / 2.142	2.141 / 2.142
f_6	2.227 / 3.000	2.126 / 2.500	f_{19}	3.792 / 2.142	4.065 / 2.142
f_7	1.716 / 1.428	1.966 / 1.666	f_{20}	2.101 / 2.142	2.115 / 2.142
f_8	1.211 / 1.428	1.333 / 1.666	f_{21}	2.195 / 3.000	2.170 / 2.500
f_9	1.000 / 2.142	1.022 / 2.142	f_{22}	4.168 / 3.000	3.767 / 2.500
f_{10}	1.291 / 1.666	1.296 / 1.666	f_{23}	2.189 / 3.000	2.046 / 2.500
f_{11}	1.411 / 2.142	1.397 / 2.142	f_{24}	2.242 / 3.000	2.104 / 2.500
f_{12}	0.984 / 2.142	0.999 / 2.142	f_{25}	1.679 / 1.428	1.377 / 2.500
f_{13}	1.276 / 1.666	1.252 / 1.666			

TABLE 5: Flow completion time (seconds) for Section. 3.2 when using TCP Cubic.

Flow	$\tau = 1$	$\tau = 4/3$	$\tau = 2$	Flow	$\tau = 1$	$\tau = 4/3$	$\tau = 2$
f_1	108	120	139	f_7	206	166	156
f_2	208	149	135	f_8	210	143	146
f_3	187	166	164	f_9	102	107	140
f_4	80	127	139	f_{10}	190	163	158
f_5	176	170	159	f_{11}	220	161	131
f_6	206	162	145	f_{12}	80	149	138
max()					220	170	164

The index value ranges from $\frac{1}{n}$ (worst case) to 1 (best case). As suggested in [15], for multi-link networks the value x_i must be normalized to an optimal fairness allocation. Throughout this paper, we normalize x_i as the ratio f_i/O_i , where f_i is the rate of flow f_i achieved through the experiments and O_i is its expected max-min fair throughput. This provides an index that qualitatively measures how closely the rates obtained from the experiments are to the theoretical rates predicted by the bottleneck structure of the network. The closer this index is to 1, the more accurate the mathematical model is to the experimental results. Table. 6 shows the Jain's fairness index we obtained for all the experiments presented in this paper (Sections. 3.3, 3.1 and 3.2).

Table. 7 presents the specific route configurations used for various experiments in Sections. 3.1 and 3.2.

Fig. A6 shows the performance of flow f_{50} in the experiment presented in Section 3.1. As expected, its performance is very similar to flow f_{25} shown in Fig. 3a.

TABLE 6: Jain’s Fairness index for all the experiments

Algorithm	3.3:Experiment 1	3.3:Experiment 2	3.3:Experiment 3
BBR	0.9926	0.9965	0.9985
Cubic	0.9353	0.9074	0.9218
Algorithm	3.1:Experiment 1	3.1:Experiment 2	
BBR	0.9954	0.9966	
Cubic	0.9077	0.8868	
Algorithm	3.2: $\tau = 1$	3.2: $\tau = 4/3$	3.2: $\tau = 2$
BBR	0.9987	0.9983	0.9939
Cubic	0.9903	0.9842	0.9957

TABLE 7: Path followed by each flow in the routing optimization experiments (Section 3.1)

Experiment 1:			
Flow	Links traversed	Flow	Links traversed
f_1	$\{l_3, l_{15}, l_{10}, l_{18}\}$	f_{14}	$\{l_7, l_8\}$
f_2	$\{l_5, l_7, l_8\}$	f_{15}	$\{l_7, l_8, l_{19}\}$
f_3	$\{l_3, l_{15}, l_{10}\}$	f_{16}	$\{l_7, l_8, l_{11}\}$
f_4	$\{l_3, l_{15}, l_{10}, l_{14}\}$	f_{17}	$\{l_{10}, l_{18}\}$
f_5	$\{l_{15}, l_{10}, l_{18}\}$	f_{18}	$\{l_{10}, l_{19}\}$
f_6	$\{l_{16}, l_8\}$	f_{19}	$\{l_{10}\}$
f_7	$\{l_{15}, l_{10}\}$	f_{20}	$\{l_{10}, l_{14}\}$
f_8	$\{l_{15}, l_{10}, l_{14}\}$	f_{21}	$\{l_8, l_9\}$
f_9	$\{l_{13}, l_6, l_{10}, l_{18}\}$	f_{22}	$\{l_8\}$
f_{10}	$\{l_{13}, l_7, l_8\}$	f_{23}	$\{l_8, l_{19}\}$
f_{11}	$\{l_{13}, l_6, l_{10}\}$	f_{24}	$\{l_8, l_{11}\}$
f_{12}	$\{l_{13}, l_6, l_{10}, l_{14}\}$	f_{25}	$\{l_{15}, l_{10}\}$
f_{13}	$\{l_7, l_8, l_9\}$		
Experiment 2:			
Flow	Links traversed	Flow	Links traversed
f_1	$\{l_3, l_{15}, l_{10}, l_{18}\}$	f_{14}	$\{l_7, l_8\}$
f_2	$\{l_5, l_7, l_8\}$	f_{15}	$\{l_7, l_8, l_{19}\}$
f_3	$\{l_3, l_{15}, l_{10}\}$	f_{16}	$\{l_7, l_8, l_{11}\}$
f_4	$\{l_3, l_{15}, l_{10}, l_{14}\}$	f_{17}	$\{l_{10}, l_{18}\}$
f_5	$\{l_{15}, l_{10}, l_{18}\}$	f_{18}	$\{l_{10}, l_{19}\}$
f_6	$\{l_{16}, l_8\}$	f_{19}	$\{l_{10}\}$
f_7	$\{l_{15}, l_{10}\}$	f_{20}	$\{l_{10}, l_{14}\}$
f_8	$\{l_{15}, l_{10}, l_{14}\}$	f_{21}	$\{l_8, l_9\}$
f_9	$\{l_{13}, l_6, l_{10}, l_{18}\}$	f_{22}	$\{l_8\}$
f_{10}	$\{l_{13}, l_7, l_8\}$	f_{23}	$\{l_8, l_{19}\}$
f_{11}	$\{l_{13}, l_6, l_{10}\}$	f_{24}	$\{l_8, l_{11}\}$
f_{12}	$\{l_{13}, l_6, l_{10}, l_{14}\}$	f_{25}	$\{l_{16}, l_8, l_{19}, l_{20}\}$
f_{13}	$\{l_7, l_8, l_9\}$		

Table. 9 presents the performance of flows f_{26} - f_{50} for the experiment described in Section. 3.1.

To construct the gradient graph of a network, only the information about a network $\mathcal{N} = \langle \mathcal{L}, \mathcal{F}, \{c_l, \forall l \in \mathcal{L}\} \rangle$ is needed. The set of flows \mathcal{F} can be obtained from traditional network monitoring tools such as NetFlow [30] or sFlow [29]. For each flow, the *GradientGraph()* procedure (Algorithm 1) needs to know the set of links it traverses. This information can also be obtained from NetFlow or sFlow provided that traffic sampling is performed at all the switches and routers of a network, as is often the case with

TABLE 8: Path followed by each flow in the fat-tree networks experiments (Section 3.2)

Flow	Experiment 1,2,3:Links traversed
f_1	$\{l_1, l_2\}$
f_2	$\{l_1, l_5, l_6, l_3\}$
f_3	$\{l_1, l_5, l_6, l_4\}$
f_4	$\{l_2, l_1\}$
f_5	$\{l_2, l_5, l_6, l_3\}$
f_6	$\{l_2, l_5, l_6, l_4\}$
f_8	$\{l_3, l_6, l_5, l_2\}$
f_9	$\{l_3, l_4\}$
f_{10}	$\{l_4, l_6, l_5, l_1\}$
f_{11}	$\{l_4, l_6, l_5, l_2\}$
f_{12}	$\{l_4, l_3\}$

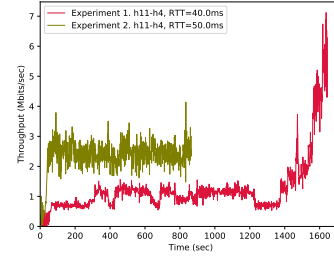


Figure A6: Acceleration of flow f_{50} by routing it through the high-bandwidth path.

TABLE 9: Experimental versus theoretical average flow transmission rate (units in Mbps).

Flow	Shortest path	Longer path	Flow	Shortest path	Longer path
f_{26}	1.513 / 1.428	1.678 / 1.666	f_{39}	1.452 / 1.666	1.443 / 1.666
f_{27}	1.580 / 1.666	1.572 / 1.666	f_{40}	1.537 / 1.666	1.636 / 1.666
f_{28}	1.449 / 1.428	1.515 / 1.666	f_{41}	1.576 / 1.666	1.564 / 1.666
f_{29}	1.523 / 1.428	1.595 / 1.666	f_{42}	1.813 / 2.142	1.855 / 2.142
f_{30}	1.327 / 1.428	1.494 / 1.666	f_{43}	1.813 / 2.142	1.903 / 2.142
f_{31}	2.605 / 3.000	2.230 / 2.500	f_{44}	1.793 / 2.142	1.824 / 2.142
f_{32}	1.249 / 1.428	1.384 / 1.666	f_{45}	1.831 / 2.142	1.852 / 2.142
f_{33}	1.340 / 1.428	1.449 / 1.666	f_{46}	2.637 / 3.000	2.182 / 2.500
f_{34}	2.203 / 2.142	2.226 / 2.142	f_{47}	2.465 / 3.000	2.108 / 2.500
f_{35}	1.536 / 1.666	1.522 / 1.666	f_{48}	2.553 / 3.000	2.158 / 2.500
f_{36}	1.924 / 2.142	1.971 / 2.142	f_{49}	2.630 / 3.000	2.235 / 2.500
f_{37}	2.065 / 2.142	2.253 / 2.142	f_{50}	1.240 / 1.428	2.359 / 2.500
f_{38}	1.520 / 1.666	1.511 / 1.666			

production networks. If that is not the case, then the set of links traversed by each flow can also be derived by looking up the routing tables, for instance using a BGP collector [16] or traceroute-like route discovery applications. The set of links \mathcal{L} and their capacity $\{c_l, \forall l \in \mathcal{L}\}$ can be derived from protocols like SNMP [31] or simply from network topology information usually available to the network operator.